

1 **Accepted version:** Ishak S., Ghannem S., Alotaibi R.M., Alkatheri R.S., Alharbi M.F., Almutrif
2 A.M., Grassi E. Semprucci F., Badraoui R., Dilara S., Hamadi N.B., Khezami L., Rudayni H.A.,
3 Boufahja F., 2025. Effects of antibiotics and metals on meiofauna assessed through
4 taxon/functional and modeling tools: a case study of amoxicillin and copper, *Marine Pollution*
5 *Bulletin*, 216, 18022. <https://doi.org/10.1016/j.marpolbul.2025.118022>.

6

7 **Effects of antibiotics and metals on meiofauna assessed through taxon/functional and**
8 **modeling tools: a case study of amoxicillin and copper**

9 **Sahar Ishak¹, Samir Ghannem¹, Renad M. Alotaibi², Rahaf S. Alkatheri², Mona F.**
10 **Alharbi², Alanood M. Almutrif², Eleonora Grassi³, Federica Semprucci³, Riadh**
11 **Badraoui⁴, Sunakbaeva Dilara⁵, Naoufel Ben Hamadi⁶, Lotfi Khezami⁶, Hassan A.**
12 **Rudayni², Fehmi Boufahja^{2,*}**

13

14 ¹ *University of Carthage, Faculty of Sciences of Bizerte, Laboratory of Environment*
15 *Biomonitoring, Coastal Ecology and Ecotoxicology Unit, 7021 Zarzouna, Tunisia.*

16 ² *Biology Department, College of Science, Imam Mohammad Ibn Saud Islamic University*
17 *(IMSIU), Riyadh 11623, Saudi Arabia.*

18 ³ *Department of Biomolecular Sciences, University of Urbino, Campus Scientifico Enrico*
19 *Mattei, Localita `Crocicchia, 61029, Urbino, Italy.*

20 ⁴ *Department of Biology, University of Ha'il, Ha'il 45851, Saudi Arabia.*

21 ⁵ *Khoja Akhmet Yassawi International Kazakh-Turkish University, Faculty of Sciences,*
22 *Department of Ecology and Chemistry, Central Campus, Turkestan, Kazakhstan*

23 ⁶ *Chemistry Department, College of Science, Imam Mohammad Ibn Saud Islamic University*
24 *(IMSIU), Box 5701, Riyadh 11432, Saudi Arabia.*

25

26 * Corresponding author. faboufahja@imamu.edu.sa (F. Boufahja)

27

28 **EMAIL ADDRESSES :**

29

30 **Sahar Ishak:** ishak-sahar@hotmail.com

31 **Samir Ghannem:** ghannemsamir7@gmail.com

32 **Renad M. Alotaibi:** 443019058@sm.imamu.edu.sa

33 **Rahaf S. Alkatheri:** 443018955@sm.imamu.edu.sa

34 **Mona F. Alharbi:** 443018894@sm.imamu.edu.sa

35 **Alanood M. Almutrif:** 438015256@sm.imamu.edu.sa

36 **Eleonora Grassi:** eleonora.grassi@uniurb.it

37 **Federica Semprucci:** federica.semprucci@uniurb.it

38 **Riadh Badraoui:** ri.badraoui@uoh.edu.sa

39 **Sunakbaeva Dilara:** dilara.sunakbayeva@ayu.edu.kz

40 **Naoufel Ben Hamadi :** nabenhamadi@imamu.edu.sa

41 **Lotfi Khezami :** lhmkhezami@imamu.edu.sa

42 **Hassan A. Rudayni:** harudayni@imamu.edu.sa

43 **Fehmi Boufahja:** faboufahja@imamu.edu.sa

44

45

46

47 **ABSTRACT**

48

49 This research examines the impacts of amoxicillin and copper, separately and together, on the
50 taxonomic and functional diversity of free-living marine nematodes. Sediment samples were
51 gathered from the Jeddah shoreline in Saudi Arabia, and meiobenthic organisms were subjected
52 to two concentrations of amoxicillin [550 and 1100 ng/L] and copper [130 mg/kg dry weight
53 (dw) and 260 mg/kg dw] in microcosms for 30 days. The findings indicated a higher nematode
54 tolerance than that of polychaetes, copepods, isopods, amphipods, and cumaceans. A notable
55 decrease in both nematode species abundance and diversity was observed as contaminant levels
56 rose, resulting in the reduction of sensitive bioindicators, specifically *Paracanthochus*
57 *sadspitensis*, *Dorylaimopsis timmi*, *Cinctonema papillata*, *Eleutherolaimus obtusicaudatus*,
58 *Terschellingia longicaudata*, *Theristus poloris*, *Halalaimus longicaudatus*, *Parodontophora*
59 *brevisetata*, and *Theristus pertenuis* for copper, as well as *C. papillata*, *T. longicaudata*, *H.*
60 *longicaudatus*, *T. pertenuis*, *D. timmi*, and *Viscosia viscosia* for amoxicillin. Conversely,
61 tolerant/opportunistic species such as *Metoncholaimus albidus* for amoxicillin and *Daptonema*
62 *oxycerca* for both copper and amoxicillin showed an increase in abundance. The pairing of
63 amoxicillin and copper demonstrated a synergistic or additive toxic impact. Furthermore,
64 pollution changed the functional characteristics of nematodes, leading to a rise in detritivore

65 species with clavate tails, and a decline in microvore species with conical and filiform tails. A
66 computational analysis also supported these findings by evaluating the toxicokinetics and
67 molecular interactions of amoxicillin and copper.

68

69 **Keywords:** Amoxicillin; Copper; Meiofauna, Taxonomic structure, Functional traits ;
70 Modeling

71

72 **1. Introduction**

73

74 The use of antibiotics, their presence in the environment, and the spread of antimicrobial
75 resistance represent a significant global health issue (Louati, 2013; Avio et al., 2015; Carvalho
76 and Santos, 2016). Antibiotics can be natural, synthetic, or semi-synthetic and possess the
77 ability to kill or inhibit the growth of microorganisms (Kummerer, 2009a). These compounds
78 are biologically active agents with antibacterial, antifungal, and antiparasitic properties,
79 designed as medications to treat bacterial infections in both humans and animals and also used
80 as food additives or for disease prevention in livestock (Kummerer, 2009b). The use of
81 pharmaceutical products in this therapeutic category has increased dramatically in recent years,
82 driven by population growth and rising demand for animal proteins, necessitating higher
83 production through growth factors and antibiotics (Zhao et al., 2019; Van Boeckel et al., 2015).
84 Consequently, antibiotics ingested by humans or animals are metabolized and excreted in
85 various active chemical forms through urine and feces into urban wastewater (Kovalakova et
86 al., 2020).

87 Antibiotic residues are also frequently detected in water bodies such as river water and
88 irrigation dam water and effluents from hospitals and sewage treatment facilities (Monteiro and
89 Boxall, 2010; Watkinson et al., 2009 ; Abera et al., 2025). They were interestingly found in
90 biological matrices such as cow urine (Abera et al., 2025) and food such as milk, lettuce, carrot,
91 and tomato (Lakew et al., 2023 ; Abera et al., 2025). The highest levels of antibiotic residues
92 found in wastewater typically range in milligrams per liter, potentially exceeding 1000 mg/L in
93 industrial areas in China and India (Larsson, 2014; O'Neill et al., 2015). Wastewater from
94 hospitals can contain small amounts of antibiotics, around a few milligrams per liter (Watkinson
95 et al., 2009). In the particular case of amoxicillin, wastewater treatment plants frequently fall
96 short in removing residues of pharmaceutical compounds, leading to its presence in ocean
97 ecosystems (Kushneet et al., 2021). Although amoxicillin has relatively low acute and chronic
98 toxicity on aquatic life forms such as *Daphnia magna*, and fish, it may still pose ecological
99 threats because of possible bioaccumulation (Sodhi et al., 2021).

100 It is recognized that when medications are introduced into aquatic ecosystems, they can
101 interact with other substances, including metals, possibly changing the physiology of non-target
102 marine and benthic species (Osorio et al., 2016). Copper is a versatile metal, with a global
103 demand in 2050 relative to 2010 likely to increase by 140% (de Koning et al., 2018; Watari et
104 al., 2021). It was found in various matrices, including soft drinks (Fanta and Sprite), food
105 supplements (commercially sold multi-mineral/vitamin tablets), and environmental water (tap
106 water and wastewater) (Tesfaye et al., 2022). Its levels in marine sediments are affected by
107 industrial operations, antifouling substances, and sediment characteristics, presenting
108 ecological hazards to marine organisms, with differing toxicity and bioavailability based on
109 sediment traits and copper forms (Yang et al., 2018). These investigations indicate that elevated
110 copper levels in water bodies lead to a notable change in prokaryotic community structure,

111 impacting biodiversity and community composition, with *D. similis* and *R. subcapitata* being
112 the most susceptible (Oliveira-Filho et al., 2004).

113 Utilizing bioindicators—organisms that facilitate the evaluation of ecosystem health—
114 allows researchers to assess the impact of pollution on the well-being and composition of living
115 organisms before a significant disruption occurs in the entire biota and ecosystem (Baldrighi et
116 al., 2019, 2021 ; Leasi et al., 2021). Meiobenthic taxa are considered bioindicators of ecosystem
117 health, especially free-living marine nematodes (Gambi et al., 2020 ; Leasi et al., 2021 ;
118 Semprucci et al., 2021). These worms make up the most diverse and populous group (60-90 %)
119 of global meiofauna and are also the most varied group inhabiting marine sediments (Ape et
120 al., 2018 ; Armenteros et al., 2019 ; Schratzberger and Somerfield, 2020; Coccozza di Montanara
121 et al., 2022). Interestingly, few studies indicate that the quantitative and qualitative features of
122 meiobenthic nematodes are significantly influenced by the presence of copper (Hedfi et al.,
123 2008) and the antibiotics penicillin G and ciprofloxacin in their immediate environment (Nasri
124 et al., 2015; 2024). Although copper's impact on free-living nematodes has been partially
125 researched at the taxonomic level (Hedfi et al., 2008), its influence on other meiobenthic groups,
126 its interaction with amoxicillin, and amoxicillin's effect on meiobenthic organisms are entirely
127 unexamined.

128 The topic investigated in this research has recently emerged as a significant global
129 concern. Thus, this research intends to address primarily the gap concerning amoxicillin, whose
130 impacts have yet to be investigated on the major meiobenthic group, nematodes. The inquiries
131 explored were: (1) Does amoxicillin negatively affect traits of meiobenthic nematodes? and (2)
132 If so, what interactions occur with copper? (3) Do nematodes exhibit taxon/functional changes
133 after their exposure to amoxicillin, copper, and their combinations? The applied experimental
134 approach was supported by several computational methods related to amoxicillin and Germ-
135 Line Development protein 3 (GLD-3) as well as the Sex-Determining Protein (SDP).

136

137 **2. Materials and methods**

138

139 *2.1. Sampling and acclimatization phase*

140 Sediment samples were collected on March 17, 2023, from an undisturbed coastal
141 location (21°14'0.07"N, 39°8'43.13"E) situated in the upper sublittoral zone along the Jeddah
142 coast, Saudi Arabia. Samples were obtained from the top 5 cm of the sediment layer, at a depth
143 of 50 cm in the water column (Hedfi et al., 2008), using Plexiglas hand cores with an internal
144 diameter of 3.6 cm and a cross-sectional area of 10 cm². This layer serves as a microhabitat that
145 exhibits the greatest taxonomic richness and abundance of meiofauna (Bin-Jumah, 2024).

146 On the sampling day, four abiotic factors were assessed at the sediment-water interface:
147 temperature and salinity were recorded with a Thermo-Salinometer (model WTW LF 196) from
148 German Wilhelm, while dissolved oxygen levels were measured using an Oxymeter (model
149 WTW OXI 330/Set), also from German Wilhelm. A pH meter (model WTW pH 330 / SET-1)
150 was employed to assess pH values. In the lab, the moisture level was ascertained by drying the
151 gathered sediment at 45°C until a constant weight was reached (Boufahja et al., 2011).
152 Subsequently, the sediment was passed through 63 µm sieves with a water jet and then dried
153 again at 45°C to analyze the sediment's grain fractions (Buchanan, 1971). Cumulative curves
154 were developed to evaluate the mean grain size, as observed by Buchanan (1971), while the
155 mass loss method at 450°C for 6 hours was used to ascertain the total organic matter content
156 (Fabiano and Danovaro, 1994).

157

158 *2.2. Selected concentrations of amoxicillin and copper*

159 The concentrations of copper in marine sediments ranged from a baseline of 30-40
160 mg/kg to a peak concentration of 1200 mg/kg (Morrisey et al., 1996; Encina-Montoya et al.,
161 2024). Additionally, standard copper concentrations vary between 4.5 and 123 mg/kg in the
162 deeper sediment layers (> 10 cm) of the ocean floor (Environment Canada, 1998). Copper
163 toxicity in marine sediments has been reported at 258 mg/kg for amphipods (Parks et al., 2018),
164 700 mg/kg for meiobenthic nematodes (Hedfi et al., 2008), and 708 mg/kg for mysids (Parks et
165 al., 2018). Two concentrations were ultimately selected for copper, 130 and 260 mg/kg dry
166 weight (dw). The lower concentration is roughly equivalent to the maximum level detected in
167 deeper, relatively unpolluted layers (>10 cm, 123 mg/kg). The highest concentration was
168 determined based on the lowest ecotoxicological level that causes toxicity in aquatic organisms
169 (258 mg/kg).

170 Many acute toxicity studies have investigated the impacts of amoxicillin on different
171 marine biological models. Nonetheless, many of them involved much shorter durations
172 compared to the typical timeframe used for meiofauna (i.e., 30 days). For instance, amoxicillin
173 exhibits a 15-minute acute toxicity level of 56.23 mg/L for the bacterium *Vibrio fischeri*
174 (Sönmez and Sivri, 2020). As an illustration, Lützhøft et al. (1999) found an EC50 of 0.0037
175 mg/L for the alga *Microcystis aeruginosa* during a 7-day exposure duration. In comparison,
176 Park and Choi (2008), along with Lee et al. (2021), reported a 48-hour EC50 value for the
177 cladocera *D. magna* that was greater than 1000 mg/L. To choose concentrations for the current
178 experiment, it was preferred to consult the environmental concentrations. Amoxicillin can be
179 detected in aquatic environments at low levels (from nanograms to micrograms per liter) (Sodhi
180 et al., 2021). For example, amoxicillin concentrations were detected in various surface water
181 bodies in the United Kingdom, Australia, and Spain, ranging from 39 to 245 ng/L (Watkinson
182 et al., 2009; Kazprzyk-Horden et al., 2007; Fatta-Kassinou et al., 2011). The presence of this
183 antibiotic was more noticeable in raw urban sewage, wastewater treatment plant influents, or

184 hospital effluents across Australia, Italy, and Spain, with levels ranging from 622 to 1670 ng/L
185 (Watkinson et al., 2009; Zuccato et al., 2010). Based on these data, two concentrations were
186 selected: 550 and 1100 ng/L. The lower concentration may represent a relatively minor
187 contamination level, as it is roughly twice the maximum environmental concentration under
188 normal circumstances (245 ng/L). The higher concentration was roughly equivalent to the
189 average within the range of 622-1670 ng/L, indicating moderate amoxicillin contamination.

190

191 *2.3. Contamination of water and sediment*

192 Amoxicillin trihydrate (Sigma Aldrich, CAS Number: 61336-70-7) was initially
193 dissolved in pre-filtered seawater (filtered using 0.7 µm pore-size Glass Microfibre filters,
194 GF/F, Whatman) without solvents, to create a 1 g/L stock solution, which was then stored in
195 dark at -20°C (de Moraes et al., 2022) until utilized for contaminating the seawater within
196 microcosms. Copper chloride dihydrate stock solutions (Sigma Aldrich, CAS Number: 10125-
197 13-0) were also prepared using the same prefiltered (0.7 µm pore-size Glass Microfibre GF/F,
198 Whatman) seawater. In the lab, the sediment designated for contamination underwent three
199 cycles of freezing at -20°C for 12 hours, followed by thawing at room temperature for 48 hours
200 to remove all life forms (Schratzberger et al., 2004). The sediment was subsequently passed
201 through a 63 µm mesh to eliminate larger particles (Boufahja et al., 2015). The copper was
202 thoroughly mixed into the sediment using a food mixer and left to equilibrate for one week at
203 4°C in the dark (Bin-Jumah, 2023). After this acclimatation period, 100 g samples of dry
204 sediment were pre-contaminated with appropriate amounts of copper and combined with 200 g
205 of natural sediment (containing live meiofauna) to reach final copper concentrations of 130 and
206 260 mg/g dw. In the control group, 100 g of azoic, uncontaminated sediment was mixed with
207 200 g of natural sediment.

208

209 *2.4. Experiment set-up*

210 The microcosms consisted of 1.5 L glass bottles (Boufahja et al., 2015), following the
211 framework followed by Badraoui et al. (2023). Each bottle contained 300 g of sediment and 1
212 liter of pre-filtered seawater (filtered through 0.7 μm pore-size Glass Microfibre filters, GF/F,
213 Whatman) obtained from the collection site (Leasi et al., 2021). These microcosms functioned
214 as closed systems, with continuous aeration throughout the experimental period provided by
215 aquarium pumps (Nasri et al., 2020).

216 A total of nine treatments were established, including one control group; two treatments
217 with copper ($\text{Cu1} = 130 \text{ mg/kg dw}$ and $\text{Cu2} = 260 \text{ mg/kg dw}$), two treatments with amoxicillin
218 ($\text{AMX1} = 550 \text{ ng/L}$ and $\text{AMX2} = 1100 \text{ ng/L}$), and four combinations of different treatments
219 (AMX1/Cu1 , AMX2/Cu2 , AMX2/Cu1 , and AMX1/Cu2). In total, 27 microcosms were set up
220 at 4°C in the absence of light, with three replicates for each treatment.

221

222 *2.5. Meiofauna study*

223 Sediment samples were preserved in a 4% buffered formaldehyde solution, with a few
224 drops of a Rose Bengal solution (0.2 g/L) added to stain meiobenthic organisms pink,
225 facilitating their distinction from inert substrate particles (Waweru et al., 2024). Meiofauna was
226 subsequently extracted from the sediments using the classic
227 levigation/resuspension/decantation method, and the biota was retained on a 40 μm sieve
228 (Rzeznik-Orignac et al., 2017). Nematode counting was performed using a 50x
229 stereomicroscope (Wild Heerbrugg model M5A), and the specimens were immersed in 10%
230 glycerol, gradually concentrated in anhydrous glycerol, and then mounted on permanent slides

231 (Bin-Jumah, 2023). Identification of genus and species was performed using a Nikon DS-Fi2
232 camera connected to a Nikon microscope, with NIS Elements Analysis Software (Version 4.0,
233 Nikon 4.00.07–build 787–64 bit). Pictorial keys by Platt and Warwick (1988) and descriptions
234 from the NeMys database (Nemys, 2024) were used for genus and species identification,
235 respectively.

236 For the analysis of functional traits, two nematode features were assessed: tail shape and
237 feeding group. Trophic groups, defined by the structure of the oral cavity, are divided into four
238 categories: epistrate grazers (2A), deposit-selective feeders (1A), non-selective feeders (1B),
239 and omnivorous predators (2B) (Wieser, 1953). Tail shape was also categorized into four types:
240 conical (co), clavate (cla), short/round (s/r), and elongated/filiform (e/f) (Semprucci et al.,
241 2018).

242

243 2.5. Computational modeling

244 This study involved examining the binding scores and molecular interactions of
245 amoxicillin with two receptors from the nematode model *Caenorhabditis elegans*, which serves
246 as a representative species for nematodes. The 3D crystal structures of GLD-3 and SDP were
247 obtained from the RCSB Protein Data Bank. GLD-3 and SDP were prepared for docking by
248 removing crystallographic water molecules, incorporating polar hydrogens, and adding
249 Kollman charges, as previously described (Ben Saad et al., 2023; Boudjema et al., 2024). Using
250 the CHARMM force field, we analyzed the interactions between amoxicillin and the receptors
251 GLD-3 and SDP to create ligand-receptor complexes, following methodologies outlined in prior
252 studies (Badraoui et al., 2023; Ishak et al., 2024; Rahmouni et al., 2024). The resulting
253 molecular interactions were recorded and characterized (Ben Saad et al., 2023; Elyousfi et al.,
254 2024; Ishak et al., 2024). We selected GLD-3 and SDP for this analysis due to their critical roles

255 in germ lineage development and sex determination in nematodes, particularly in *C. elegans*
256 (Badraoui et al., 2023; Ishak et al., 2024).

257

258 *2.7. Data processing*

259 In this study, various biodiversity indices were assessed for free-living marine
260 nematodes using PRIMER version 5.0 software. The faunal parameters comprised total
261 abundance, species number, Margalef's species richness, and the Shannon-Wiener index ($H'e$).
262 One-way ANOVA alongside Tukey's HSD tests was employed to compare the treatments. The
263 Chi-square test was employed to evaluate variations in relative abundances among different
264 functional groups after $\sqrt{}$ -transformation. Three multivariate analyses were conducted. Non-
265 metric multidimensional scaling (nMDS) diagrams were generated based on both species
266 abundance and functional traits, applying square root transformations and calculating Bray-
267 Curtis similarity coefficients (Bray and Curtis, 1957). The analysis of similarity (ANOSIM)
268 was used to evaluate changes in the taxonomic and functional composition of nematode groups
269 among the different treatments. In addition, similarity percentages (SIMPER) analysis was
270 carried out to determine the contribution of individual species or functional groups to the
271 observed dissimilarities among treatments (Clarke, 1993).

272

273 **3. Results**

274

275 *3.1. Abiotic traits of the collection site*

276 The standard depth for collecting sediment was 50 cm. The measured temperature was
277 34.6 °C, whereas the dissolved oxygen concentration was 9.21 mg/l. Furthermore, it was
278 observed that the recorded salinity and pH levels were 41.45 PSU and 8.4, respectively. The
279 gathered sediment had $9.62 \pm 0.71\%$ silt/clay particles (smaller than 63 μm) and $90.38 \pm 0.71\%$
280 coarse particles (larger than 63 μm). The sandy fraction showed a median particle size of 283
281 $\pm 22 \mu\text{m}$, a moisture level of $19.63 \pm 2.17\%$, and an organic matter content of $7.04 \pm 0.92\%$

282

283 *3.2. Abundance of meiobenthic organisms*

284 Nematodes, along with the next five dominant groups (polychaetes, copepods, isopods,
285 amphipods, and cumaceans), constituted the meiobenthos collected from the sampling site (see
286 Table 1). Nonetheless, since the nematofauna was the primary focus of the present experiment,
287 more detailed analyses were restricted to this phylum. Table 1 illustrates the changes in
288 nematode abundance following exposure to amoxicillin and/or copper. The total nematode
289 abundance was significantly lower in all treatments compared to the control (Tukey-HSD test:
290 p-values < 0.05), with the most pronounced reductions observed in AMX2/Cu2, AMX2, and
291 AMX2/Cu1.

292 Furthermore, pairwise comparisons of abundance between combined treatments
293 (AMX2/Cu2 and AMX1/Cu1) and single treatments (Cu1, Cu2, AMX1, and AMX2) indicated
294 that combined exposures had a more substantial impact than the individual application of
295 copper and amoxicillin (see Table 1). A similar trend was observed for the other meiobenthic
296 groups, whose populations also declined—in many cases more markedly than nematodes
297 (Tukey HSD test, Table 1). Notably, a complete absence of certain taxa occurred in 2 to 6 out
298 of the 8 treatments involving copper and amoxicillin. The most affected group was amphipods,

299 which were absent following exposure to AMX1, AMX2, AMX1/Cu1, AMX2/Cu2,
300 AMX2/Cu1, and AMX1/Cu2.

301

302 3.3. Taxonomic diversity of meiobenthic nematodes

303 The nematode community comprised 25 species belonging to 5 orders and 13 families
304 (Table 2). The dominant order was Monhysterida, with Xyalidae being the most represented
305 family. After the experiment, the species *Eleutherolaimus obtusicaudatus* was the most
306 abundant in the control assemblage, accounting for $8.59 \pm 0.78\%$ of the total community. This
307 species was eliminated in certain treatments (AMX2/Cu2), while in others (AMX1/Cu2), its
308 abundance increased relative to the control (see Table 3). Similarly, *Cinctonema papillata* was
309 prevalent in the control group, comprising $7.27 \pm 2.98\%$; but was absent in the AMX2 and
310 AMX2/Cu1 treatments and exhibited minimal presence in AMX2/Cu2 ($0.52 \pm 0.91\%$) (Table
311 3).

312 It is noteworthy that some species present in the control were completely eliminated at
313 higher concentrations and in combined treatments. These include *Daptonema oxycerca*
314 (AMX2/Cu2 and AMX2/Cu1), *Halalaimus longicaudatus* (AMX1), *Metoncholaimus albidus*
315 (AMX1/Cu2 and AMX2/Cu1), *Terschellingia communis* (AMX2/Cu2 and AMX2/Cu1), and *T.*
316 *longicaudata* (AMX1/Cu1 and AMX2/Cu2). Conversely, certain species initially found in low
317 abundance in the control became prevalent at higher concentrations and under combined
318 exposures. Notable examples include *Desmodora pontica* in treatments AMX2/Cu2 and
319 AMX2/Cu1, and *M. albidus*, in AMX2/Cu2 (refer to Table 3).

320 Figure 1 illustrates a significant reduction in taxonomic richness in the AMX2/Cu2,
321 AMX2, AMX2/Cu1, and AMX1/Cu2 treatments (Tukey's HSD test: $p < 0.0001$). For other
322 diversity indices, notable differences (Tukey's HSD test) were noted, including Margalef's (p -

323 value = 0.031) and the Shannon-Wiener (p -value = 0.046) indices, between AMX2/Cu2 and the
324 control (see Fig. 1).

325 Figure 2 presents the clustering analysis and nMDS ordination, demonstrating the
326 impact of AMX and Cu contamination on species distribution (Stress = 0.12). As a result, three
327 distinct groups were identified: (1) Group 1, consisting solely of AMX2/Cu2, represents the
328 assemblages most dissimilar to the control nematofauna; (2) Group 2, represented by
329 AMX2/Cu1 and AMX2, includes assemblages closest to the control replicates; and (3) Group
330 3 comprises the control assemblage along with the remaining treatments.

331 As shown in Table 3, the SIMPER analysis indicated that nine species
332 (*Paracanthochus sadspitensis*, *Dorylaimopsis timmi*, *C. papillata*, *E. obtusicaudatus*, *T.*
333 *longicaudata*, *Theristus polaris*, *H. longicaudatus*, *Parodontophora beviseta*, and *Theristus*
334 *pertenuis*) were the primary contributors to the dissimilarity observed between control and
335 copper treatments; all of these species exhibited a decline in abundance.

336 Similarly, six species showed reduced abundance after exposure to amoxicillin
337 compared to the controls: *C. papillata*, *T. longicaudata*, *H. longicaudatus*, *T. pertenuis*, *D.*
338 *timmi*, and *Viscosia viscosia*. Conversely, certain species showed increased abundance under
339 specific treatments. In the case of copper, *D. oxycerca* increased in abundance, while under
340 the lowest amoxicillin concentration (AMX1), *T. communis*, *D. oxycerca*, *M. albidus*, and
341 *Ptycholaimellus sindhicus* were more abundant.

342 The degree of taxonomic changes varied among treatments (see Table 4). The highest
343 dissimilarity values compared to the controls were observed in AMX2/Cu2 (54.53%),
344 AMX2/Cu1 (41.04%), and AMX2 (39.33%). All other treatments resulted in 19.37% to 29.18%
345 dissimilarity compared to the uncontaminated control (UC). Finally, it was observed that

346 increasing concentrations of both copper and amoxicillin were associated with higher average
347 dissimilarity values.

348

349 *3.4. Functional traits of meiobenthic nematodes*

350 Following the experiment, nematodes from groups 1B and 1A were the most abundant
351 in the control samples, accounting for $49.69 \pm 1.38\%$ and $19.12 \pm 2.22\%$ of the total
352 nematofauna, respectively. Significant changes were observed as a result of contamination by
353 amoxicillin, copper, or their combinations (refer to Fig. 3). Cluster analysis combined with the
354 nMDS ordination revealed a separation into three categories: Group 1, consisting solely of the
355 AMX2/Cu2 treatment, was the most distinct from the control assemblage, Group 2, which
356 included Cu1, Cu2, UC, AMX1, AMX1/Cu2, AMX1, and AMX1/Cu1; and Group 3, composed
357 of AMX2/Cu1 and AMX2, which occupied an intermediate position on the ordination plot.

358 Most treatments resulted in a decrease in the abundance of group 1A, as shown by the
359 SIMPER analysis (see Table 5 and Fig. 3). This decline was responsible for the differences
360 observed in 6 of the 8 treatments (Cu1, Cu2, AMX1, AMX2, AMX1/Cu1, and AMX1/Cu2)
361 relative to the controls. Conversely, the trophic shifts in five treatments (Cu1, AMX2,
362 AMX2/Cu2, AMX1/Cu2, and AMX2/Cu1) showed an increase in the proportion of group 2B.
363 To a lesser extent, increases in trophic group 1B also contributed to the trophic differences in
364 three treatments: Cu2, AMX1, and AMX2/Cu2.

365 The extent of trophic variation differed among treatments (refer to Table 4). The highest
366 values compared to the controls were noted for AMX2/Cu2 (63.26%), AMX2 (26.54%), and
367 AMX2/Cu1 (26.54%). All remaining treatments resulted in only 8.79 to 19.90% taxonomic
368 variation relative to UC. As in previous observations, increasing concentration was associated
369 with higher average dissimilarity values for both copper and amoxicillin (refer to Table 4).

370 Nematodes with conical and clavate tails were the most prevalent in the control group,
371 with relative abundances of $47.02 \pm 3.53\%$ and $37.65 \pm 1.79\%$, respectively. Cluster analysis
372 and the nMDS ordination (Fig. 3) identified three groups of assemblages: Group 1 (AMX2/Cu2
373 and AMX2/Cu1), Group 2 (UC, AMX1/Cu2, Cu1, AMX1, and AMX1), and Group 3 (UC
374 together with the other treatments).

375 SIMPER analysis (Table 5) revealed a reduction in the relative abundance of conical
376 tails in all contaminated treatments except AMX1/Cu2. Conversely, all treatments showed an
377 increase in the proportion of clavate tails, along with a decline in the occurrence of nematodes
378 with elongated/filiform tails (see Table 5). The treatments AMX2/Cu2 (26.37%) and
379 AMX2/Cu1 (24.60%) showed the highest average dissimilarity compared to the controls,
380 indicating an overall increase in dissimilarity with rising contamination levels of both copper
381 and amoxicillin (refer to Table 5).

382 The second-stage nMDS (see Fig. 4) indicated that trophic groups were significantly
383 influenced by contamination (90.039%), while tail shape was comparatively less impacted
384 (83.126%).

385

386 3.5. Computational findings

387 The binding affinities of amoxicillin for GLD-3 and SDP are presented in Table 6,
388 showing negative docking of -6.4 and -7.7 kcal/mol, respectively. It was initially anticipated
389 that amoxicillin would form at least four conventional hydrogen bonds; however, it formed six
390 typical hydrogen bonds with SDP. Specifically, it interacted three times with LYS82, and once
391 each with GLN175, ASP166, and GLN78. The hydrogen bonds formed with GLD-3 were
392 accompanied by a π -Alkyl interaction with ARG113 (refer to Figs. 5 and 6). Our research
393 indicates that amoxicillin is precisely positioned ($<2.5 \text{ \AA}$) within the binding sites of both GLD-

394 3 and SDP, with interaction distances of 1.994 and 1.875 Å, respectively, to the nearest
395 interacting residues of the receptors.

396

397 **4. Discussion**

398

399 The objective of this study was to evaluate the impact of amoxicillin [550 ng/L (AMX1)
400 and 1100 ng/L (AMX2)] or copper [130 mg/kg dry weight (dw) (Cu1) and 260 mg/kg dw
401 (Cu2)], and their combined mixtures (AMX1/Cu1, AMX2/Cu2, AMX1/Cu2, and AMX2/Cu1)
402 on the abundance of meiofauna, and taxonomic and functional diversity of nematodes collected
403 from the Jeddah coast, Saudi Arabia.

404

405 *4.1. How did the presence of meiobenthic organisms alter under stress exposure?*

406 A general decline in meiobenthic organisms was observed following exposure to copper
407 and/or amoxicillin, with the most significant impact on nematodes occurring under the highest
408 concentrations of amoxicillin, particularly in AMX2/Cu2, AMX2, and AMX2/Cu1.

409 Overall, copper is commonly associated with reduced population densities and elevated
410 mortality rates in aquatic species like fungi (*Clavariopsis aquatica*), zooplankton (*Mytilinia*
411 sp.), and macroinvertebrates (*Gammarus pulex*), potentially inducing behavioral changes
412 (Environment Canada, 1998; Sandrine et al., 2009). In general, meiobenthic organisms are
413 affected by stressors either through direct exposure to contaminated sediments or *via* ingestion
414 of polluted particles (Armynot du Châtelet et al., 2016; Lassoued et al., 2025). It has been
415 demonstrated that both dissolved and particulate forms of copper in seawater can be readily
416 absorbed by sediments, whether bound to drugs and organic matter or not (Hung et al., 2024).

417 Alternatively, several indirect mechanisms may help explain the observed decline in
418 meiobenthic taxa. For example :

419 (1) The accumulation of dead bodies from sensitive benthic species can reduce sediment
420 porosity and increase adhesion (Allouche et al., 2025), thereby hindering the
421 movement of meiobenthos for reproduction and feeding (Hedfi et al., 2008;
422 Allouche et al., 2020), particularly impacting crustaceans and polychaetes that have
423 a flattened body, presenting a large surface area exposed to xenobiotics.

424 (2) Bashir et al. (2020) reported that the disposal of copper mine tailings in the ocean
425 led to the degradation of the coastal marine environments by decreasing light
426 penetration and photosynthetic activity, resulting in increased mortality among
427 algae, invertebrates, and fish.

428 (3) Finally, chronic exposure to copper in marine sediments have been shown to caused
429 DNA damage and elevated mortality in the polychaete *Alitta virens* (Watson et al.,
430 2018).

431 In general, the polychaetes, copepods, isopods, amphipods, and cumaceans appear
432 to be the most vulnerable taxa, likely due to the high number of setae on their bodies,
433 which impairs movement in such sticky, contaminated substrates (Sbrocca et al.,
434 2021; Schratzberger et al., 2023).

435 At this stage, it becomes essential to investigate the effects of amoxicillin, copper, and
436 their combinations on the taxonomic diversity of free-living marine nematodes, in order to
437 distinguish between sensitive indicator species and tolerant ones.

438

439 *4.2. How do nematodes react to stress from a taxonomic standpoint?*

440 Significant declines in diversity indices and/or species richness were observed
441 particularly in treatments AMX2/Cu2, AMX2, AMX2/Cu1, and AMX1/Cu2 (see Fig. 1). This
442 reduction is undoubtedly attributable to the detrimental effects of these pollutants on sensitive
443 species. Hedfi et al. (2008) reported a marked reduction in the taxonomic diversity of
444 meiobenthic nematodes along the Bizerte shores (Tunisia), associated with increasing copper
445 levels in marine sediments. More broadly, Environment Canada (1998) and Lee and Correa
446 (2007) also recorded diversity loss in benthic invertebrates and meiofauna following exposure
447 to copper or mine tailings. Regard amoxicillin, it has been shown to negatively affect aquatic
448 organisms within the food web, particularly cyanobacteria, which are more sensitive than green
449 algae (Andreozzi et al., 2004; González-Pleiter et al., 2013). Moreover, amoxicillin may
450 stimulate *M. aeruginosa* proliferation and microcystin production, potentially leading to
451 harmful algal blooms (Liu et al., 2016).

452 After exposure to copper, the species *P. sadspitensis*, *D. timmi*, *C. papillata*, *E.*
453 *obtusicaudatus*, *T. longicaudata*, *T. poloris*, *H. longicaudatus*, *P. beviseta*, and *T. pertenuis*
454 could be considered as sentinel species, due to distinct sensitivity. The epistrate feeder
455 *Paracanthochus sadspitensis* and *D. timmi* were particularly affected, likely due to the decline
456 in diatoms, their main food source. This finding is consistent with Sandrine et al. (2009), who
457 reported increased mortality in the diatom *Cocconeis* sp. at copper concentrations above 25
458 $\mu\text{g.L}^{-1}$. In contrast, *D. oxycerca* increased in abundance under high copper concentrations
459 compared to the controls, suggesting a tolerance or adaptation to metal-enriched conditions.
460 This may be linked to its ability to consume macrophyte remains (Grassi et al., 2023; Coccozza
461 di Montanara et al., 2024). Sandrine et al. (2009) also suggested that copper contamination may
462 enhance the growth of certain macrophytes, such as *Callitriche platycarpa*. Moreover, non-
463 selective deposit feeders may benefit from feeding on decaying organic matter derived from
464 sensitive taxa (Allouche et al., 2025).

465 Similarly, exposure to amoxicillin negatively affected six species: *C. papillata*, *T.*
466 *longicaudata*, *H. longicaudatus*, *T. pertenuis*, *D. timmi*, and *V. viscosia*. This is likely linked to
467 amoxicillin's mechanism of action, which reduces bacterial availability for the microvorous
468 species such as *C. papillata*, *T. longicaudata*, and *H. longicaudatus*. Nasri et al. (2015) observed
469 significant shifts in both taxonomic and trophic composition in a Mediterranean benthic
470 community exposed to penicillin G under laboratory conditions. In contrast, some species, such
471 as *D. oxycerca* and *M. albidus*, appeared as opportunistic/tolerant taxa for amoxicillin. This is
472 consistent with their trophic roles as obligate or facultative detritivores.

473 The most pronounced impacts on nematode taxonomic composition were observed in
474 the combined and high-concentration treatments, particularly AMX2/Cu2 (see Fig. 1 and Table
475 4). This was further supported by the nMDS ordination, which showed a clear separation
476 between single and combined treatments. Under mixed exposures to copper and amoxicillin,
477 several species, including *E. obtusicaudatus*, *T. pertenuis*, *T. longicaudata*, *H. longicaudatus*,
478 and *Trissonchulus oceanus*, disappeared. The latter species may shift toward detritivory when
479 organic matter from dead organisms is present (Moens et al., 2006). This finding is supported
480 by reductions in the populations of other species such as *C. papillata*, *T. polaris*, *Daptonema*
481 *conicum*, *Paramonhystra pellucida*, *P. beviseta*, and *Sabatieria falcifera*. These results suggest
482 a potential synergistic or additive effect of amoxicillin and copper on taxonomic composition
483 of meiobenthic nematodes. The dissimilarity values supports this hypothesis (refer to Table 4),
484 as they were notably higher in the high-concentration mixture compared to single treatments or
485 the control. Several studies support the idea of synergistic interactions between copper and
486 amoxicillin. For instance, copper has been shown to enhance the antibacterial activity of
487 amoxicillin (Khashan et al., 2015; Nleonu et al., 2022; Su et al., 2024). Su et al. (2024)
488 demonstrated that the co-application of amoxicillin and copper during composting reduced
489 humification, with stronger negative effects when used together than individually. Copper-

490 amoxicillin complexes were found to be more effective against *Staphylococcus aureus* than
491 amoxicillin alone (Nleonu et al., 2022). Likewise, copper oxide nanoparticles showed strong
492 antibacterial effects against *E. coli* and *S. aureus*, with enhanced efficacy when combined with
493 amoxicillin (Khashan et al., 2015).

494

495 4.3. How do nematodes react to stress from a functional standpoint?

496 Examining functional traits offers essential insight into ecotoxicological responses,
497 although this aspect is often overlooked by meiobenthic nematologists (Semprucci et al., 2022;
498 Allouche et al., 2025). At the conclusion of the present bioassay, the greatest dissimilarities in
499 feeding were observed between contaminated treatments and controls, particularly in combined
500 treatments at higher concentrations (AMX2/Cu2 and AMX2/Cu1). Similarly, the most
501 significant changes in tail morphotypes were also recorded under these same conditions.

502 In these treatments, predators (2B) were found in higher proportions, possibly indicating
503 that the effects of amoxicillin and copper became more pronounced toward the later phase of
504 the experimental. These worms are known to feed fresh dead prey (Moens et al., 2002; Allouche
505 et al., 2021 a,b), suggesting that mortality among other taxa may have provided an abundant
506 food source. Additionally, nematodes with clavate-shaped tails became more prevalent, whereas
507 those with conical or elongated/filiform tails generally declined or disappeared. This is
508 consistent with the idea that conical-tailed nematodes, which rely on a broader base to leap and
509 move, are more exposed to contaminants adsorbed onto sediment particles (Bellakhal et al.,
510 2023). Meanwhile, nematodes with elongated tails face difficulties in foraging under sticky and
511 compacted sediment conditions, which are characteristic of contaminated environments.

512 The second-stage nMDS ordination (refer to Fig. 4) confirmed that the distribution of
513 nematode species following exposure to amoxicillin and/or copper was primarily associated

514 with their buccal cavity, and to a lesser degree with tail shape. Notably, microvorous nematodes
515 were among the most affected groups. Amoxicillin, in fact, has been shown to significantly
516 impact aquatic ecosystems, with cyanobacteria being especially vulnerable, as evidenced in
517 conventional ecotoxicological bioassays (González-Pleiter et al., 2013; Kovaláková et al.,
518 2020). For instance, amoxicillin is harmful to the *Cyanobacterium anabaena* CPB4337, while
519 it does not affect the green alga *Pseudokirchneriella subcapitata* (González-Pleiter et al., 2013),
520 and may even stimulate its photosynthetic activity (Liu et al., 2016). This pattern helps explain
521 the relatively high abundance of obligate (1B) and facultative (2B) herbivorous nematodes,
522 which may have benefited from altered microbial and primary producer communities resulting
523 from amoxicillin exposure.

524

525 *4.4. Is there support from computational modeling for both taxonomic and functional traits?*

526 Table 6 presents the binding affinities of amoxicillin to GLD-3 and SDP. The results
527 indicated negative scores, with satisfactory binding affinities of -6.4 for GLD-3 and -7.7
528 kcal/mol for SDP. Negative binding energies, particularly those below -6.0 kcal/mol, are
529 frequently associated with biologically relevant effects (Allouche et al., 2022; Ishak et al.,
530 2024). Given that hydrogen bonds play a fundamental role in mediating biological activity
531 (Badraoui et al., 2024; Elyousfi et al., 2024), it was hypothesized that amoxicillin would
532 establish at least four conventional hydrogen bonds. In practice, it formed six hydrogen bonds
533 when bound to SDP, interacting three times with LYS82 and once with each of GLN175,
534 ASP166, and GLN78. In case of GLD-3, the established hydrogen bonds were accompanied by
535 a π -alkyl interaction with ARG113 (Figures 5 and 6). Hydrogen bonding and other non-covalent
536 interactions are recognized as critical determinants of the toxicological effects of several
537 compounds, including antibiotics (Ishak et al., 2024; Ben Amor et al., 2025). Our results showed

538 that amoxicillin was tightly embedded within the active sites of both GLD-3 and SDP, with
539 interaction distances of 1.994 Å and 1.875 Å, respectively, to the nearest binding residues. Such
540 close molecular embedding is known to enhance the biological activity and stability of ligand–
541 receptor complexes (Ben Amor et al., 2025; Rahmouni et al., 2024; Elyousfi et al., 2024). The
542 strong molecular interaction of amoxicillin with these two nematode receptors provides a
543 mechanistic explanation that supports the experimentally observed reduction in taxonomic
544 diversity and species prevalence, especially under high concentrations and in combination with
545 copper.

546

547 **5. Conclusions**

548 This study evaluated the effects of amoxicillin, copper, and their mixtures on
549 meiobenthic organisms, with a particular focus on nematodes. A notable decrease in
550 meiobenthic abundance was observed, alongside a significant decline in taxonomic diversity,
551 especially under elevated concentrations and combined exposures. Some species emerged as
552 indicators of pollution, including *D. oxycerca* (for copper) and *M. albidus* (for both). In
553 contrast, several taxa were recognized as sensitive species: *P. sadspitensis*, *D. timmi*, *C.*
554 *papillata*, *E. obtusicaudatus*, *T. longicaudata*, *T. polaris*, *H. longicaudatus*, *P. beviseta*, and *T.*
555 *pertenuis* for copper, and *C. papillata*, *T. longicaudata*, *H. longicaudatus*, *T. pertenuis*, *D.*
556 *timmi*, and *V. viscosia* for amoxicillin. The results further confirmed the higher sensitivity of
557 polychaetes and crustaceans compared to nematodes to both contaminants, and highlighted the
558 presence of synergistic/additive effects between these two chemicals. These interactions may
559 be explained by electrostatic affinities between the two substances, potentially enhancing their
560 toxicological impact.

561 In summary, the research underscores the negative consequences of pharmaceutical and
562 metal contamination on meiobenthic biodiversity, emphasizing the need for further targeted

563 studies. Future research should employ mono-species bioassays, focusing on sensitive
564 nematode taxa exposed to amoxicillin and/or copper, and should include detailed assessments
565 of mortality, morphotyping, and genetic haplotyping.

566

567 **Acknowledgments**

568 This work was supported and funded by the Deanship of Scientific Research at Imam
569 Mohammad Ibn Saud Islamic University (IMSIU) (grant number IMSIU-DDRSP2502).

570 **Conflict of interest:** On behalf of all authors, the corresponding author states that there is no
571 conflict of interest.

572 **Ethical approval:** Not applicable.

573 **Consent for publications:** The Author grants the Publisher the sole and exclusive license of
574 full copyright.

575 **Consent to participate:** All authors read and approved the final version of the manuscript being
576 submitted.

577 **Data availability:** The data supporting this study's findings are available from the
578 corresponding author upon reasonable request.

579

580 **References**

581

582 Abera, S., Yaya, E.E., Chandravanshi, B.S., 2025. Development of HPLC-DAD method for the
583 separation and simultaneous determination of ten antibiotic residues in food and

584 environmental samples using surface floating organic droplet-based air-assisted
585 liquid-liquid micro-extraction. J. Chromatogr. A 1748, 465817.
586 <https://doi.org/10.1016/j.chroma.2025.465817>

587 Allouche, M., Al-Shomrani, A.M.A., Bagilb, F.S., Alajmi, R.F., Bin-Jumah, M.N. Alqhtani,
588 H.A., Pacioglu, O., Hedfi, A., Abd-Elkader, O.H., Boufahja, F., 2025. Are irbesartan
589 and losartan ecotoxic for free-living marine nematodes? Response elements from
590 taxonomic and functional features, Reg. Stud. Mar. Sci. 81, 103934.

591 Allouche, M., Ishak, S., Ali, M., Amor, H., Almalki, M., Karachle, P., Harrath, A. H. Abu-Zied,
592 R., Badraoui, R., Boufahja, F., 2022. Molecular Interactions of Polyvinyl Chloride
593 Microplastics and Beta-Blockers (Diltiazem and Bisoprolol) and Their Effects on
594 Marine Meiofauna: Combined in vivo and Modeling Study. J. Hazard. Mater. 431.
595 [10.1016/j.jhazmat.2022.128609](https://doi.org/10.1016/j.jhazmat.2022.128609).

596 Allouche, M., Nasri, A., Harrath, A.H., Mansour, L., Alwasel, S., Beyrem, H., Plávan, G.,
597 Rohal-Lupher, M., Boufahja, F., 2021a. Meiobenthic nematode *Oncholaimus*
598 *campyloceroides* as a model in laboratory studies: selection, culture, and
599 fluorescence microscopy after exposure to phenanthrene and chrysene. Environ. Sci.
600 Pollut. Res. 28(23), 29484–29497.

601 Allouche, M., Nasri, A., Harrath, A.H., Mansour, L., Alwasel, S., Beyrem, H., Plávan, G.,
602 Rohal-Lupher, M., Boufahja, F., 2021b. Meiobenthic nematode *Oncholaimus*
603 *campyloceroides* as a model in laboratory studies: selection, culture, and
604 fluorescence microscopy after exposure to phenanthrene and chrysene. Environ. Sci.
605 Pollut. Res. 28, 29484-29497.

606 Andreozzi, R., Caprio, V., Ciniglia, C., De Champdoré, M., Lo Giudice, R., Marotta, R.,
607 Zuccato, E., 2004. Antibiotics in the environment: occurrence in Italian STPs, fate,

608 and preliminary assessment on algal toxicity of amoxicillin. Environ. Sci. Technol.
609 38 (24), 6832-8.

610 Ape, F., Gristina, M., Chemello, R., Sarà, G., Mirto, S., 2018. Meiofauna associated with
611 vermetid reefs: the role of macroalgae in increasing habitat size and complexity.
612 Coral Reefs 37(3), 875–889.

613 Armenteros, M., Pérez-García, J.A., Marzo-Pérez, D., Rodríguez-García, P., 2019. The
614 influential role of the habitat on the diversity patterns of free-living aquatic nematode
615 assemblages in the Cuban archipelago. Diversity. 11(9), 166.

616 Armynot du Châtelet E., Bout-Roumazeilles V., Coccioni R., Frontalini F., Francescangeli F.,
617 Margaritelli G., Rettori R., Spagnoli F., Semprucci F., Trentesaux A., Tribovillard
618 N. 2016. Environmental control on a land-sea transitional setting – Integrated
619 microfaunal, sedimentological, and geochemical approaches. Environ. Earth Sci, 75,
620 123.

621 Avio, C.G., Gorbi, S., Milan, M., Benedetti, M., Fattorini, D., d' Errico, G., Pauletto, M.,
622 Bargelloni, L., Regoli, F., 2015. Pollutants bioavailability and toxicological risk from
623 microplastics to marine mussels. Environ. Pollut. 198, 211e222.

624 Badraoui R, Gargouri M, Brahmi F, Ben-Nasr H, Bahrini I, Soussi A. 2024. Protective effects
625 of Juglans regia oil on lead acetate-induced reprotoxicity in rats: an antioxidant,
626 histological and computational molecular study. J. Sci. Food. Agric.
627 <https://doi.org/10.1002/jsfa.14024>.

628 Badraoui, R., Allouche, M., El Ouaer, D., Siddiqui, A.J., Ishak, S., Hedfi, A., Beyrem, H.,
629 Pacioglu, O., Rudayni, H.A., Fehmi Boufahja., 2023. Ecotoxicity of chrysene and
630 phenanthrene on meiobenthic nematodes with a case study of *Terschellingia*

631 *longicaudata*: Taxonomics, toxicokinetics, and molecular interactions modelling,
632 Environ. Pollut. 316 (1), 120459. <https://doi.org/10.1016/j.envpol.2022.120459>.

633 Baldrighi, E., Vasapollo, C., Grassi, E., Alvisi, F., Cesaroni, L., Balsamo, M., Semprucci, F.,
634 2021. Meiobenthic assemblages as ecological indicator of natural variability induced
635 by ecosystem engineers. Reg. Stud. Mar. Sci., 45, 101824.

636 Baldrighi E., Semprucci F., Franzo A., Cvitkovic I, Bogner D., Despalatovic M., Berto D.,
637 Malgorzata Formalewicz M., Scarpato A., Frapiccini E., Marini M., Grego M., 2019.
638 Meiofaunal communities in four Adriatic ports: Baseline data for risk assessment in
639 ballast water management. Mar. Pollut. Bull. 147, 171-184.

640 Bashir, I., Lone, F.A., Bhat, R.A., Mir, S.A., Dar, Z.A., Dar, S.A., 2020. Concerns and Threats
641 of Contamination on Aquatic Ecosystems. Bioremediat. Biotechnol. 27, 1–26.

642 Bellakhal, M., Ishak, S., Al-Hoshani, N., Qurtam, A.A., Al-Zharani, M., Pacioglu, O., et al.,
643 2023. The multifaceted effects of fluoranthene and polystyrene on the taxonomic
644 composition and associated functional traits of marine meiofauna, by using single
645 and mixture applications. Mar. Pollut. Bull. 194, 115390.

646 Ben Amor, B., Hamdaoui, L., Daoud, S., Ammar, M., Louati, N., Elleuch, A., et al., 2025.
647 Impact of Sub-Chronic Exposure to Kalach on male reproductive system and sperm
648 function: In Silico Modelling and In Vivo Study in Rats. Reprod. Toxicol. 108853.

649 Ben Saad, H., Frikha, D., Bouallegue, A., Badraoui, R., Mellouli, M., Kallel, H., et al., 2023.
650 Mitigation of Hepatic Impairment with Polysaccharides from Red Alga *Albidum*
651 *corallinum* Supplementation through Promoting the Lipid Profile and Liver
652 Homeostasis in Tebuconazole-Exposed Rats. Pharmaceuticals. 16(9), 1305.

653 Bin-Jumah, M.N., 2023. Do functional traits and biochemical biomarkers of the nematode
654 *Oncholaimus campylocercoides* De Coninck and Schuurmans Stekhoven, 1933
655 affected by fluoranthene and polystyrene microplastics? Results from a microcosm
656 bioassay and molecular modeling. Mar. Pollut. Bull. 194(Pt B), 115294.

657 Bin-Jumah, M.N., 2024. Are anticoagulant drugs ecotoxic for meiobenthic nematodes from
658 Saudi Arabia? First data on taxon/functional diversity and computational evidences.
659 Mar. Pollut. Bull. 200, 116029.

660 Boudjema, K., Chouala, K., Khelef, Y., Chenna H, Badraoui R, Boumendjel M, et al., 2025.
661 Antioxidant Effects of *Moringa oleifera* Against Abamectin-Induced Oxidative
662 Stress in the Brain and Erythrocytes of Rats. Chem. Biodivers. e202402709-
663 e202402709.

664 Boufahja, F., Ismaily, S., Beyrem, H., 2015. Experimental evidence of effects of an antimetabolic
665 agent, Colchicine, on a nematode community through a microcosm approach. Cah.
666 Biol. Mar. 56, 39-48.

667 Bray, J.R., Curtis, J.T., 1957. An ordination of the upland forest communities of southern
668 Wisconsin. Ecol. Monogr. 27, 325–349.

669 Buchanan, J.B., 1971. Measurement of the physical and chemical environment: Sediments. In:
670 N.A. Holme & A.D. McIntyre (eds). Methods for the Study of Marine Benthos.
671 International Biological Programme Handbook No. 16. Blackwell Scientific
672 Publications, Oxford, 334 pp.

673 Carvalho, Je., Santos, L., 2016. Les antibiotiques en milieu aquatique: retour sur le scénario
674 européen. Environ. Int. 736-757. ISSN 0160-4120.
675 <https://doi.org/10.1016/j.envint.2016.06.025>.

676 Cipurković, A., Marić, S., Horozić, E., Husejnagić, D., Cipurković, S., 2023. Copper (II)
677 complexes with some antibiotics: synthesis, FT-IR study and in vitro antibacterial
678 activity. *Int. J. Adv. Chem.*

679 Clarke, K.R., 1993. Non-parametric multivariate analyses of changes in community structure.
680 *Aust. J. Ecol.* 18, 117–143.

681 Cocozza di Montanara A., Baldrighi E., Franzo A., Catani L., Grassi E., Sandulli R., Semprucci
682 F., 2022. Free-living nematodes research: State of the art, prospects, and future
683 directions. A bibliometric analysis approach. *Ecol. Inform.* 72, 101891.

684 Cocozza di Montanara, A., Baldrighi, E., López Correa, M., Chianese, E., Appolloni, L.,
685 Simoncini, N., Sandulli, R., Zeppilli, D., Semprucci, F., Gambi, M.C., Donnarumma,
686 L. 2024. Meiobenthos and ocean acidification: effects on meiobenthic communities
687 inhabiting Mediterranean cold shallow CO₂-vents. *Estuar. Coast. Shelf Sci.* 300,
688 108730

689 De Koning, A., Kleijn, R., Huppes, G., Sprecher, B., Van Engelen, G., 2018. Metal supply
690 constraints for a low-carbon economy? *Resour. Conserv. Recycl.* 129, 202-208.

691 de Moraes, A.C., Orlando, E.D., da Rosa Prado, E.J., de Carvalho, A.C.C., Machado-Neto,
692 J.G., Colnaghi Simionato, A.V., Eberlin, M.N., de Andrade Belo, M.A., 2022.
693 Ecotoxicological assessment of amoxicillin trihydrate: Stability, solubility, and
694 acute toxicity for *Oreochromis niloticus*, *Lemna minor*, and *Daphnia magna*. *Clean.*
695 *Chem. Eng.* 1, 100005.

696 De Oliveira-Filho, E., Lopes, R., Paumgarten, F., 2004. Comparative study on the susceptibility
697 of freshwater species to copper-based pesticides. *Chemosphere.* 56 (4), 369-74.

698 Dinh, Q.T., Alliot, F., Moreau-Guigon, E., Eurin, J., 2011. Chevreuil, M., Labadie, P.
699 Measurement of trace levels of antibiotics in river water using on-line enrichment
700 and triple-quadrupole LC-MS/MS. *Talanta*. 85, 1238–1245. doi:
701 10.1016/j.talanta.2011.05.013.

702 Elyousfi, S., Ishak, S., Beyrem, H., Al-Hoshani, N., Abd-Elkader, OH, Pacioglu O, et al., 2024.
703 Experimental exposure of bivalves (*Ruditapes decussatus*) and meiobenthos
704 (*Metoncholaimus pristiurus*) to 2, 2' 4, 4'-tetrabromodiphenyl ether (PBDE-47)
705 assessed biochemical, computational modeling, and microbial tools. *Mar. Pollut.*
706 *Bull.* 209, 117191.

707 Encina-Montoya, F., Ramírez-Sánchez, E., Oberti-Grassau, C., Gallardo, C., Arias-Melgarejo,
708 C., Esse, C., Mulsow, S., Mejias-Lagos, P., Vega-Aguayo, R., 2024. Historical trend
709 of ecological risk caused by copper sediment in Quintero Bay, Chile, associated with
710 a copper smelter and refinery. *Mar. Pollut. Bull.* 211, 117410.

711 Environnement Canada., 1998. Canadian sediment quality guidelines for copper: Supporting
712 document. Service de la conservation de l'environnement, Direction générale de la
713 science des écosystèmes, Direction de la qualité de l'environnement et de la politique
714 scientifique, Division des recommandations et des normes, Ottawa. Ébauche.

715 Fatta-Kassinos, D., Meric, S., Nikolau, A., 2011. Pharmaceutical residues in environmental
716 waste and wastewater: current state of knowledge and future research. *Anal. Bioanal.*
717 *Chem.* 399, 251–275.

718 Gambi, C., Dell'Anno, A., Corinaldesi, C., Lo Martire, M., Musco, L., Da Ros, Z., Armiento,
719 G., Danovaro, R., 2020. Impact of historical contamination on meiofaunal
720 assemblages: The case study of Bagnoli-Coroglio Bay (southern Tyrrhenian Sea).
721 *Mar. Environ. Res.* 156, 104907.

722 González-Pleiter, M., Gonzalo, S., Rodea-Palomares, I., Leganés, F., Rosal, R., Boltes, K.,
723 Marco, E., Fernández-Piñas, F., 2013. Toxicity of five antibiotics and their mixtures
724 towards photosynthetic aquatic organisms: implications for environmental risk
725 assessment. *Water. Res.* 47 (6), 2050-64.

726 Grassi E., Catani L, Magni P., Gravina M.F., Semprucci F., 2023. Taxonomic and functional
727 diversity of nematode fauna: two sides of the same coin in the ecological quality
728 assessment of transitional environments. *Estuar. Coast. Shelf Sci.* 295, 108550.

729 Hedfi, A., Mahmoudi, E., Beyrem, H., Boufahja, F., Essid, N., Aïssa, P., 2008. Réponse d'une
730 communauté de nématodes libres marins à une contamination par le cuivre: Étude
731 microcosmique. *Bull. Soc. Zool. Fr.* 133, 97-106.

732 Hung, M.-Y., Huang, W.-H., Tsai, H.-C., Hsieh, C.-Y., Chen, T.-C., 2024. Copper Distribution
733 and Binding Affinity to Size-Fractioned Dissolved and Particulate Organic Matter in
734 River Sediment. *Environments.* 11, 129.

735 Ishak, S., Allouche, M., Alotaibi, G.S., Alwthey, N.S., Al-Subaie, R.A., Al-Hoshani, et al.,
736 2024. Experimental and computational assessment of Antiparkinson Medication
737 effects on meiofauna: Case study of Benserazide and Trihexyphenidyl. *Mar. Pollut.*
738 *Bull.* 205, 116668. <https://doi.org/10.1016/j.marpolbul.2024.116668>.

739 Kazprzyk-Horden, B., Dinsdale, R., Guwy, A., 2007. Multiresidue method for the formation of
740 basic/neutral pharmaceuticals and illicit drugs in surface water solid-phase extraction
741 and ultra performance liquid chromatography-positive Electro spray ionization
742 tandem mass spectrometry. *J. Chromatogr. A.* 1161, 132–145.

743 Khashan, K., Sulaiman, G., Abdulameer, F., 2015. Synthesis and Antibacterial Activity of CuO
744 Nanoparticles Suspension Induced by Laser Ablation in Liquid. *Arab. J. Sci. Eng.*
745 41, 301-310.

746 Kovalakova, P., Cizmas, L., McDonald, T.J., Marsalek, B., Feng, M., Sharma, V.K. 2020.
747 Occurrence and toxicity of antibiotics in the aquatic environment: A review.
748 Chemosphere. 251, 126351. <https://doi.org/10.1016/j.chemosphere.2020.126351>.

749 Kümmerer, K., 2009 (a). Antibiotics in the aquatic environment – A review – Part I.
750 Chemosphere. 75(4), 417-434. <https://doi.org/10.1016/j.chemosphere.2008.11.086>.

751 Kümmerer, K., 2009(b). Antibiotics in the aquatic environment – A review – Part I.
752 Chemosphere, 75(4), 417-434. <https://doi.org/10.1016/j.chemosphere.2008.11.086>.

753 Kushneet, K.S., Mohit, K., Dileep, K.S., 2021. Insight into the amoxicillin resistance,
754 ecotoxicity, and remediation strategies, J. Water Process. Eng. 39, 101858.
755 <https://doi.org/10.1016/j.jwpe.2020.101858>.

756 Lakew, A., Megersa, N., Chandravanshi, B.S., 2023. Validation of modified QuEChERS
757 extraction method for quantitative enrichment of seven multiclass antibiotic residues
758 from vegetables followed by RP-LC-UV analysis. Heliyon 9, e15227.
759 <https://doi.org/10.1016/j.heliyon.2023.e15227>

760 Lassoued, A., Boufahja, F., Plavan, G., Ben Hamadi, N., Ali, M.A.M., Elfalleh, W., Badraoui,
761 R., Bendif, H., Hedfi, A., 2025. An Experimental Study to Assess the Ecotoxicity of
762 Warfarin and Tinzaparin on Meiobenthic Amphipods: Original Taxonomic Data from
763 Saudi Arabia and Computational Modeling. Toxics. 13, 264.
764 <https://doi.org/10.3390/toxics13040264>

765 Larsson, D.G.J., 2014. Pollution from drug manufacturing: review and perspectives. Philos.
766 Trans. R. Soc. B Biol. Sci.

767 Leasi, F., Sevigny, J.L., Hassett, B.T., 2021. Meiofauna as a valuable bioindicator of climate
768 change in the polar regions, Ecol. Indic. 121, 107133.

- 769 Lee, M., Correa, J., 2007. An assessment of the impact of copper mine tailings disposal on
770 meiofaunal assemblages using microcosm bioassays.. *Mar. Environ. Res.* 64 (1). 1-
771 20. <https://doi.org/10.1016/J.MARENRES.2006.11.001>.
- 772 Lee, S., Kim, C., Liu, X., Lee, S., Kho, Y., Kim, W.K., Kim, P., Choi, K., 2021. Évaluation des
773 risques écologiques de l'amoxicilline, de l'enrofloxacin et de la néomycine: leurs
774 concentrations actuelles dans l'environnement d'eau douce sont-elles sans danger?
775 *Toxics*. 9(8), 196. DOI: 10.3390/Toxics9080196.
- 776 Liu, Y., Chen, S., Zhang, J., Gao, B., 2016. Growth, microcystin-production and proteomic
777 responses of *Microcystis aeruginosa* under long-term exposure to amoxicillin. *Water*.
778 *Res.* 93, 141-152.
- 779 Louati, H., 2013. Etude de la biorémediation de sédiments contaminés par des hydrocarbures
780 aromatiques polycycliques: impact écologique sur la microflore et la méiofaune de la
781 lagune de Bizerte. *Ecologie, Environnement*. Université Montpellier II Sciences et
782 Techniques du Languedoc. Faculté des sciences de Bizerte (Tunisie). Français. NNT :
783 2013MON20118. tel-01023058
- 784 Lützhøft, H.H., Halling-Sørensen, B., Jørgensen, S.E., 1999. Algal toxicity of antibacterial
785 agents applied in danish fish farming. *Arch. Environ. Contam. Toxicol.* 36, 1–6. doi:
786 10.1007/s002449900435.
- 787 Moens, T., Luyten, C., Middelburg, J.J., Herman, P.M.J., Vincx, M., 2002. Tracing organic
788 matter sources of estuarine tidal flat nematodes with stable carbon isotopes. *Mar.*
789 *Ecol. Prog. Ser.* 234, 127–137.

790 Moens, T., Bergtold, M., Traunspurger, W., 2006. Feeding ecology of free-living benthic
791 nematodes. In: Abebe E, Andrassy I, Traunspurger W, eds. Freshwater Nematodes:
792 Ecology and taxonomy. Wallingford: CAB International: 752.

793 Monteiro, S.C., Boxall, A.B., 2010. Occurrence and fate of human pharmaceuticals in the
794 environment. *Rev. Environ. Contam. Toxicol.* 202, 53-154. doi: 10.1007/978-1-
795 4419-1157-5_2.

796 Morrisey, D., Underwood, A., Howitt, L., 1996. Effects of copper on the faunas of marine soft-
797 sediments: An experimental field study. *Mar. Biol.* 125, 199-213.

798 Nasri, A., Jouili, S., Boufahja, F., Hedfi, A., Mahmoudi, E., Aïssa, P., Essid, N., Beyrem, H.,
799 2015. Effects of increasing levels of pharmaceutical penicillin G contamination on
800 structure of free living nematode communities in experimental microcosms. *Environ.*
801 *Toxicol. Pharmacol.* 40(1), 215-219.

802 Nasri, A., Hannachi, A., Allouche, M., Hamouda, B., Mahmoudi, E., 2024. Is Changing in
803 Feeding-Groups Nematode as an Indicator of an Ecosystem Disturbed by
804 Ciprofloxacin/Bde-47 Combined Exposure? *Ann. environ. sci. Toxicol.* 6. 2637-
805 5338. 10.22259/2637-5338.0602002.

806 Nemys, 2024. Nemys: World Database of Nematodes. Available online at:
807 <https://nemys.ugent.be>.

808 Nleonu, E.C., Ezeibe, A.U., Nwafor, I.A., Nnaoma, I.E., 2022. Ligating Properties and
809 Antimicrobial Studies of Metal (II) Complexes of Amoxicillin. *Haya Saudi J. Life.*
810 *Sci.* 7(2), 66-69.

811 O'Neill et al., 2015. Securing new drugs for future generations: the pipeline of antibiotics. *Rev.*
812 *Antimicrob. Resist.* 20, 1-16.

813 Osorio, V., Larrañaga, A., Aceña, J., Pérez, S., Barceló, D., 2016. La concentration et le risque
814 des produits pharmaceutiques dans les systèmes d'eau douce sont liés à la densité de
815 population et aux unités de bétail dans les rivières ibériques. *Sci. Total Environ.* 540,
816 267–277. DOI : 10.1016/j.scitotenv.2015.06.143.

817 Parks, A., Cashman, M., Perron, M., Portis, L., Cantwell, M., Katz, D., Ho, K., Burgess, R.
818 2018. Magnitude of acute toxicity of marine sediments amended with conventional
819 copper and nanocopper. *Environ. Toxicol. Chem.* 37.

820 Park, S., Choi, K. Hazard assessment of commonly used agricultural antibiotics on aquatic
821 ecosystems. 2008. *Ecotoxicology.* 17, 526–538. doi: 10.1007/s10646-008-0209-x.

822 Platt, M., Warwick, R. M. 1988. *Free-Living Marine Nematodes: Part II, British Chromadorids.*
823 Cambridge Univ.Press, Cambridge, UK.

824 Rahmouni, F., Hamdaoui, L., Saoudi, M., Badraoui, R., Rebai, T., 2024. Antioxidant and
825 antiproliferative effects of *Teucrium polium* extract: Computational and in vivo study
826 in rats. *Toxicol. Mech. Methods.* 34(5), 495-506.

827 Rzeznik-Orignac, R., Boucher, G., Fichet, D., Richard, P., 2008. Stable isotope analysis of food
828 source and trophic position of intertidal nematodes and copepods. *Mar. Ecol. Prog.*
829 *Ser.* 359, 145-150.

830 Rzeznik-Orignac, J., Kalenitchenko, D., Mariette, J.J., Bodiou, J-Y., Le Bris, N., Derelle, E.,
831 2017. Comparison of meiofaunal diversity by combined morphological and
832 molecular approaches in a shallow Mediterranean sediment. *Marine Biology*, 2017,
833 164 (3), 40.

834 Sandrine, J., Anne, Morin., Eric, T., 2009. Effet du cuivre sur la structure et le fonctionnement
835 des écosystèmes aquatiques. *L'Act. Chim.* 334, pp.55-58. (ineris-00963195).

836 Sbrocca, C., De Troch, M., Losi, V., Grassi, E., Balsamo, M., Semprucci, F., 2021. Habitat-
837 diversity relations between sessile macrobenthos and benthic copepods in the rocky
838 shores of a Marine Protected Area. *Water*, 13, 1020.

839 Schratzberger, M., Danovaro, R., Ingels, J., Montagna, P., Rohal Luper, M., Semprucci, F.,
840 Somerfield, P. 2023. Hidden Players—Meiofauna Mediate Ecosystem Effects of
841 Anthropogenic Disturbances in the Ocean. In: Giere, O., Schratzberger, M. (eds) *New*
842 *Horizons in Meiobenthos Research*. Springer, Cham. 175–255 pp.
843 https://doi.org/10.1007/978-3-031-21622-0_7.

844 Schratzberger, M., Somerfield, P.J., 2020. Effects of widespread human disturbances in the
845 marine environment suggest a new agenda for meiofauna research is needed. *Sci.*
846 *Total Environ.* 728(4), 138435.

847 Schratzberger, M., Warr, K., Rogers, S.I., 2007. Functional diversity of nematode communities
848 in the southwestern North Sea. *Mar. Environ. Res.* 63, 368-389.

849 Schratzberger, M., Whomersley, P., Warr, K., Bolam, S.G., Rees, H.L., 2004. Colonisation of
850 various types of sediment by estuarine nematodes via lateral infaunal migration: a
851 laboratory study. *Mar. Biol.* 145, 69-78.

852 Semprucci, F., Cesaroni, L., Guidi, L., Balsamo, M., 2018. Do the morphological and functional
853 traits of free-living marine nematodes mirror taxonomical diversity? *Mar Environ*
854 *Res.* 135, 114-122.

855 Semprucci, F., Grassi, E., Balsamo, M., 2022. Simple is the best: an alternative method for the
856 analysis of free-living nematode assemblage structure. *Water*, 14, 1114.

857 Semprucci, F., Appolloni, L., Grassi, E., Donnarumma, L., Cesaroni, L., Tirimberio, G.,
858 Chianese, E., Di Donato, P., Russo, G.F., Balsamo, M., Sandulli R. 2021. Antarctic

859 Special Protected Area 161 as a Reference to Assess the Effects of Anthropogenic
860 and Natural Impacts on Meiobenthic Assemblages. *Diversity* 13, 626.

861 Semprucci, F., Facca, C., Ferrigno, F., Balsamo, M., Sfriso, A., Sandulli, R., 2019. Biotic and
862 abiotic factors affecting seasonal and spatial distribution of meiofauna and
863 macrophytobenthos in transitional coastal waters. *Estuar. Coast. Shelf Sci.* 219: 328–
864 340.

865 Sekar, R., Kailasa, S., Chen, Y., Wu, H., 2014. Electrospray ionization tandem mass
866 spectrometric studies to probe the interaction of Cu (II) with amoxicillin. *Chinese*
867 *Chem. Lett.* 25, 39-45.

868 Sodhi, K., Kumar, M., Singh, D., 2021. Insight into the amoxicillin resistance, ecotoxicity, and
869 remediation strategies. *J. Water. Process. Eng.* 39, 101858.

870 Sönmez, V., Sivri, N., 2020. The Toxic Effects of Commonly Used Antibiotics in Turkey on
871 Aquatic Organisms. *J. Anatol. Environ. Anim. Sci.*

872 Su, Y., Zhou, L., Zhuo, Q., Fang, C., You, J., Han, L., Huang, G., 2024. Microbial mechanisms
873 involved in negative effects of amoxicillin and copper on humification during
874 composting of dairy cattle manure. *Bioresour. Technol.* 130623.

875 Tesfaye, E., Chandravanshi, B.S., Negash, N., Tessema, M., 2022. Development of a new
876 electrochemical method for the determination of copper(II) at trace levels in
877 environmental and food samples, *RSC Adv.* 12, 35367-35382.
878 <https://doi.org/10.1039/D2RA06941E>

879 Van Boeckel, T.P., Brower, C., Gilbert, M., Grenfell, B.T., Levin, S.A., Robinson, T.P., Teillant,
880 A., Laxminarayan, R., 2015. Global trends in antimicrobial use in food animals. *Proc.*

881 Natl. Acad. Sci. U S A. 2015 May 5. 112(18), 5649-54. doi:
882 10.1073/pnas.1503141112.

883 Vanaverbeke, J. T. N., Bezerra, Braeckman, U. A., De Groote, N., De Meester, T., Deprez, S.,
884 Derycke, P., Gilarte, K., Guilini, F., Hauquier, L., Lins, T., Maria, T., Moens, E., Pape,
885 N., Smol, M., Taheri, J., Van Campenhout, A., Vanreusel, X., Wu, M., Vincx., 2015.
886 NeMys: World Database of Free-Living Marine Nematodes.

887 Watari, T., Nansai, K., Nakajima, K., 2021. Major metals demand, supply, and environmental
888 impacts to 2100: A critical review. *Resour. Conserv. Recycl.* 164, 105107.

889 Watkinson, A.J., Murby, E.J., Kolpin, D.W., Costanzo, S.D., 2009. The occurrence of antibiotics
890 in an urban watershed: from wastewater to drinking water. *Sci. Total. Environ.*
891 407(8), 2711-2723. doi: 10.1016/j.scitotenv.2008.11.059.

892 Watson, G., Pini, J., Richir, J., 2018. Chronic exposure to copper and zinc induces DNA damage
893 in the polychaete *Alitta virens* and the implications for future toxicity of coastal sites.
894 *Environ. pollut.* 243, 1498-1508.

895 Waweru, B.W., Wanjohi, C.W., Muthumbi, C.W., Gichuki, N.N., Eric Okuku., 2024. Meiofauna
896 as bioindicators of organic and inorganic pollution of estuarine sediments in Kenya.
897 *WIO J. Mar. Sci.* 23(1), 69-80.

898 Wieser, W., 1959. Die Beziehung zwischen Mundhöhlengestalt, Ernährungsweise und
899 Vorkommen bei freilebenden marinen Nematoden. *Arkiv. För. Zoologi.* 1953, 2, 439–
900 484.

901 Yang, J., Jeppe, K., Pettigrove, V., Zhang, X., 2018. Environmental DNA Metabarcoding
902 Supporting Community Assessment of Environmental Stressors in a Field-Based
903 Sediment Microcosm Study. *Environ. Sci. amp; Technol.* 52 (24), 14469-14479.

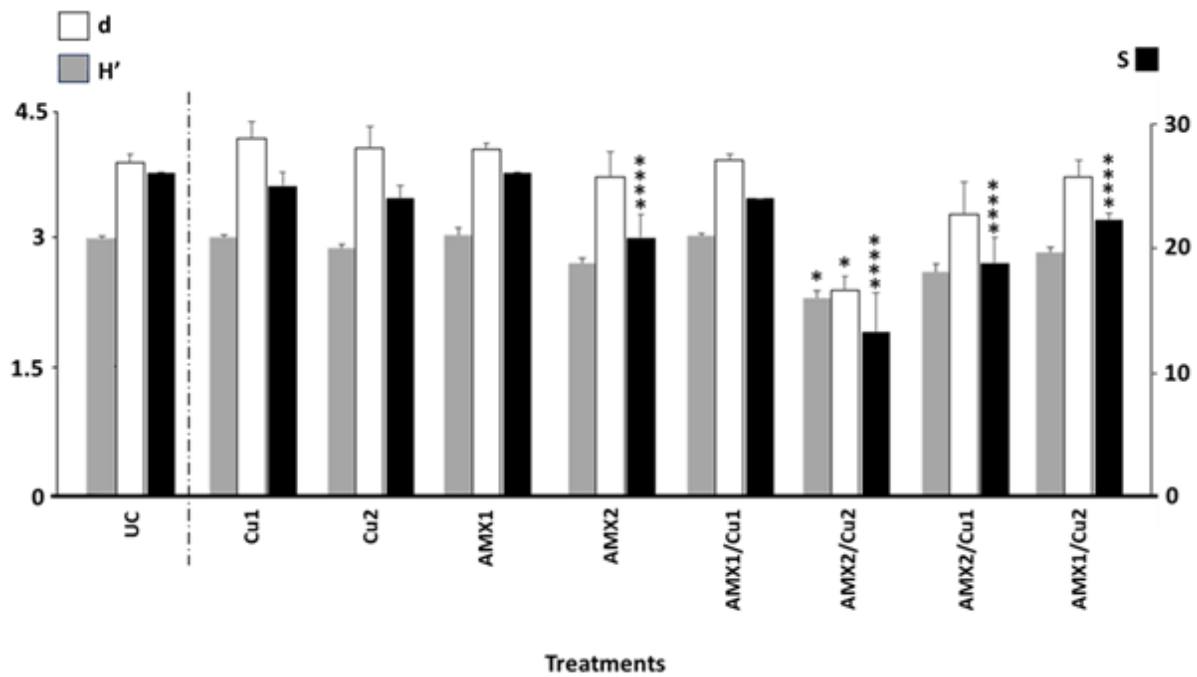
904 Zermane, M., Berkani, M., Teniou, A., Aminabhavi, T., Vasseghian, Y., Catanante, G., Lakhdari,
905 N., Rhouati, A., 2024. Modeling approach for Ti₃C₂ MXene-based fluorescent
906 aptasensor for amoxicillin biosensing in water matrices. *J. Environ. Manage.* 360,
907 121072.

908 Zhao, Y., Cocerva, T., Cox, S., Tardif, S., Su, J.Q., Zhu, Y.G., Brandt, K.K., 2019. Evidence for
909 co-selection of antibiotic resistance genes and mobile genetic elements in metal
910 polluted urban soils, *Sci. Total. Environ.* 656, 512-520, ISSN 0048-9697,
911 <https://doi.org/10.1016/j.scitotenv.2018.11.372>.

912 Zuccato, E., Castiglioni, S., BagnatiR, MelisM, FanelliR., 2010. Source, occurrence and fate of
913 antibiotics in the Italian aquatic environment. *J. Hazard. Mater.* 179, 1042–1048.

914

915



916

917 **Fig. 1.** Graphical representation of univariate indices for nematode communities from the control treatment (UC)
918 and in treatments enriched with amoxicillin [550 ng/L (AMX1) and 1100 ng/L (AMX2)], copper [130 mg/kg Dry
919 Weight 'dw' (Cu1) and 260 mg/kg dw (Cu2)] and their mixtures (AMX1Cu1, AMX2Cu2, AMX2Cu1, and
920 AMX1Cu2). Taxonomic indices: H' = Shannon-Wiener index, d = Margalef's, species richness, S = species
921 number. Tukey's HSD test : $p < 0.05$ (*), $p < 0.0001$ (***).

922

923

924

925

926

927

928

929

930

931

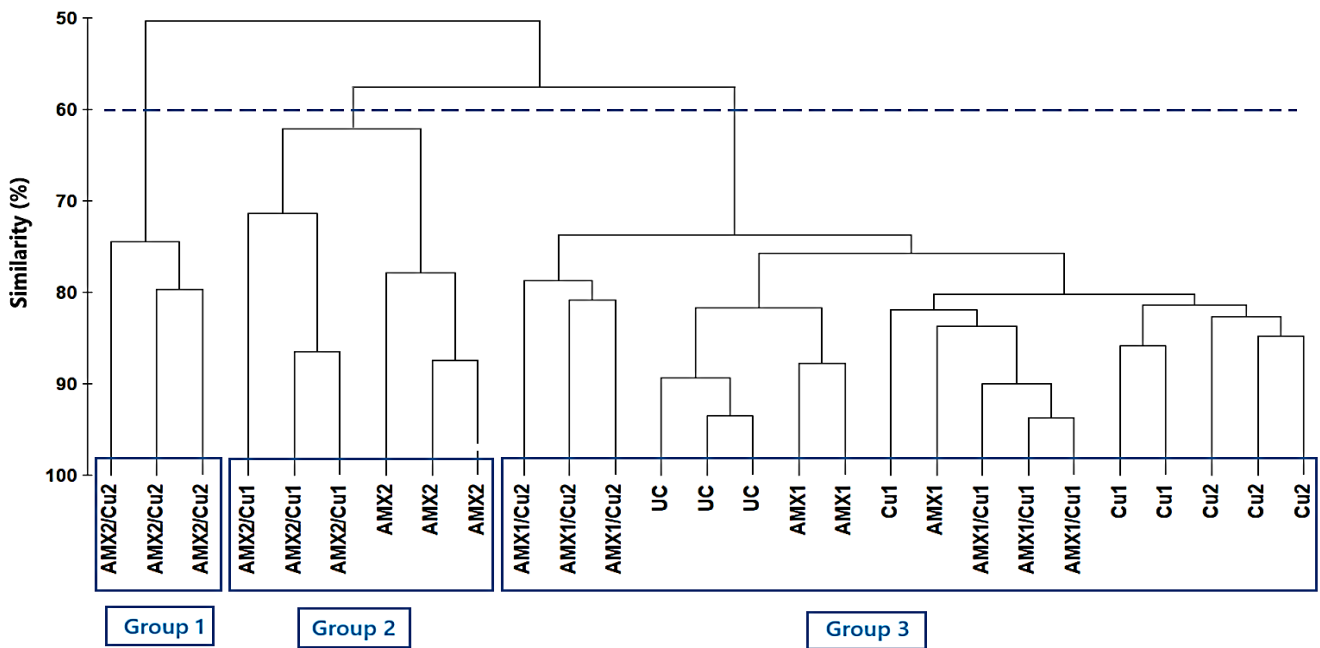
932

933

934

935

936



937

938

939

940

941

942

943

944

945

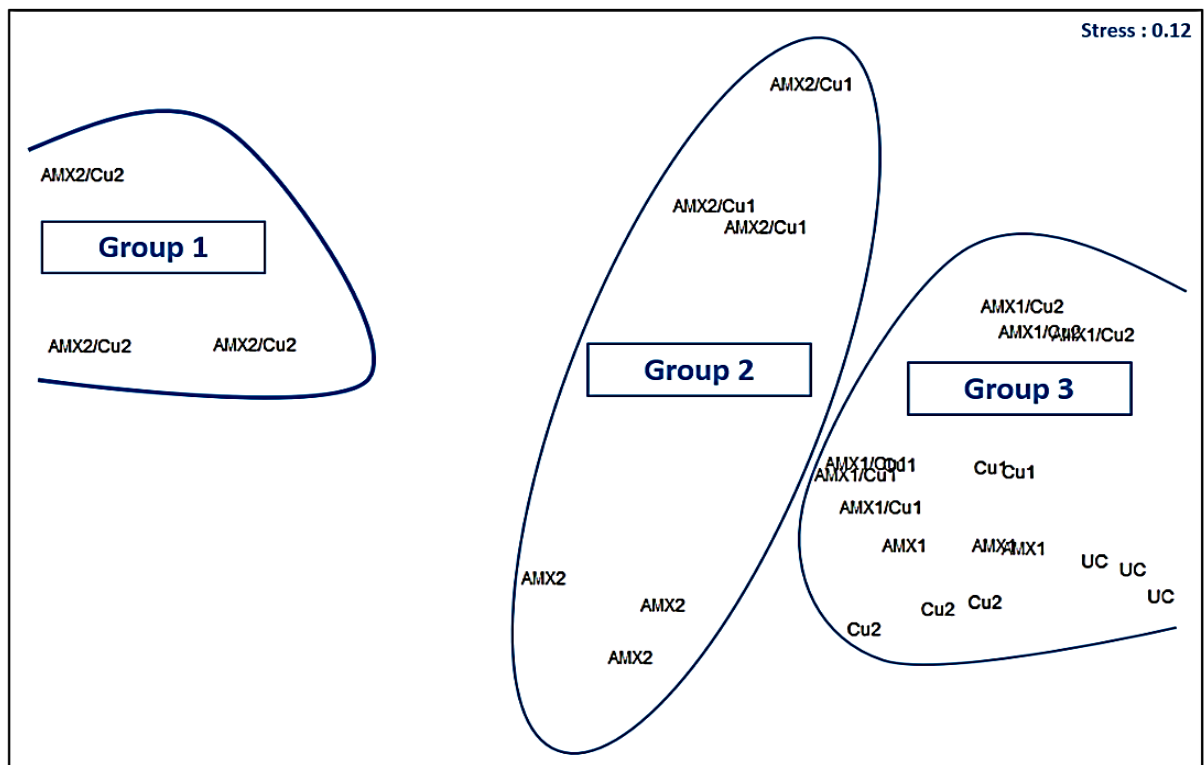
946

947

948

949

950



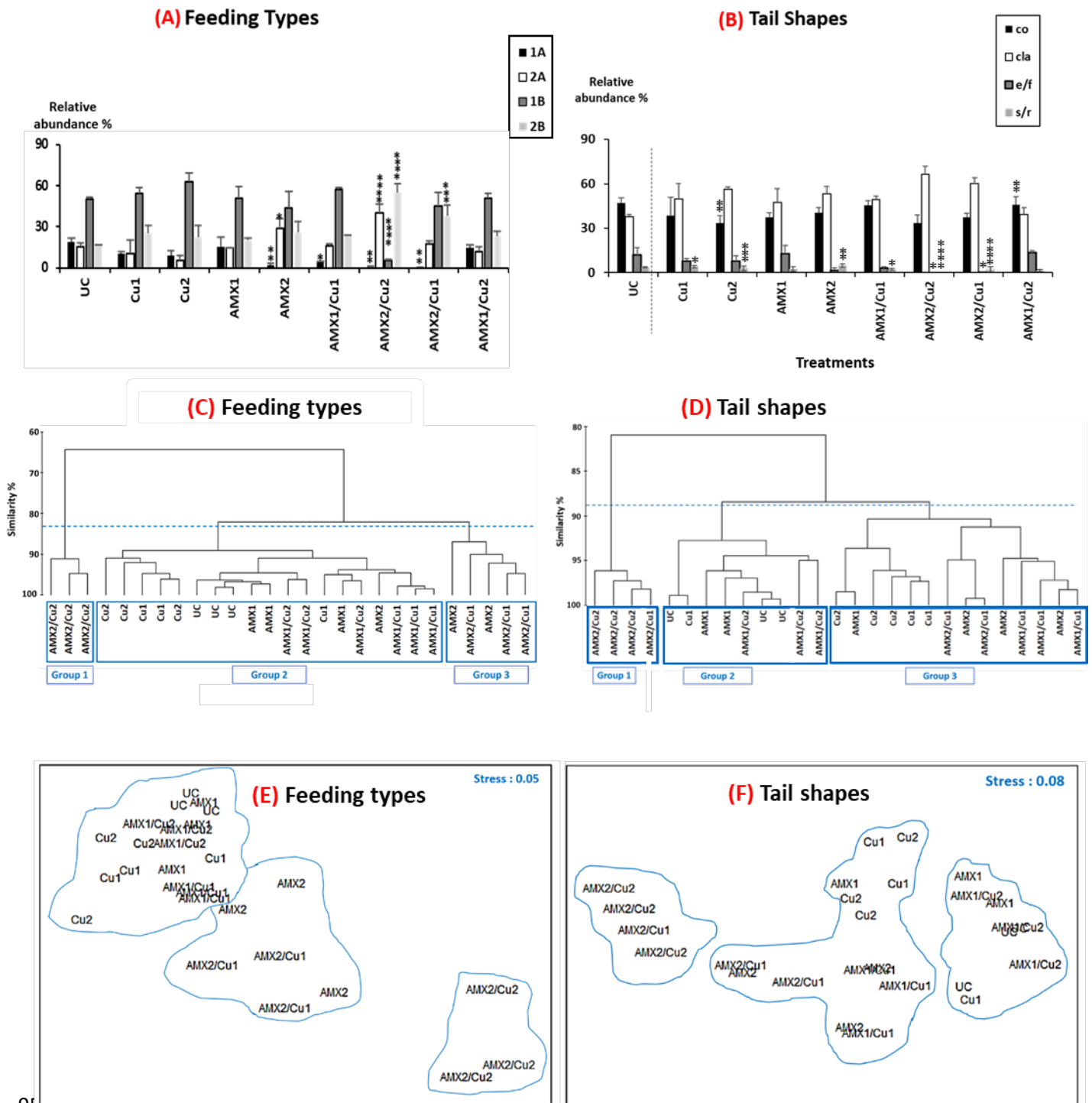
951

952

Fig. 2. Two-dimensional non-metric multidimensional scaling (nMDS) plot based on nematode species composition from the control treatment (UC) and treatment enriched with amoxicillin [550 ng/L (AMX1) and 1100

953 ng/L (AMX2)], copper [130 mg/kg Dry Weight 'dw' (Cu1) and 260 mg/kg dw (Cu2)] and their mixtures
 954 (AMX1Cu1, AMX2Cu2, AMX2Cu1, and AMX1Cu2).

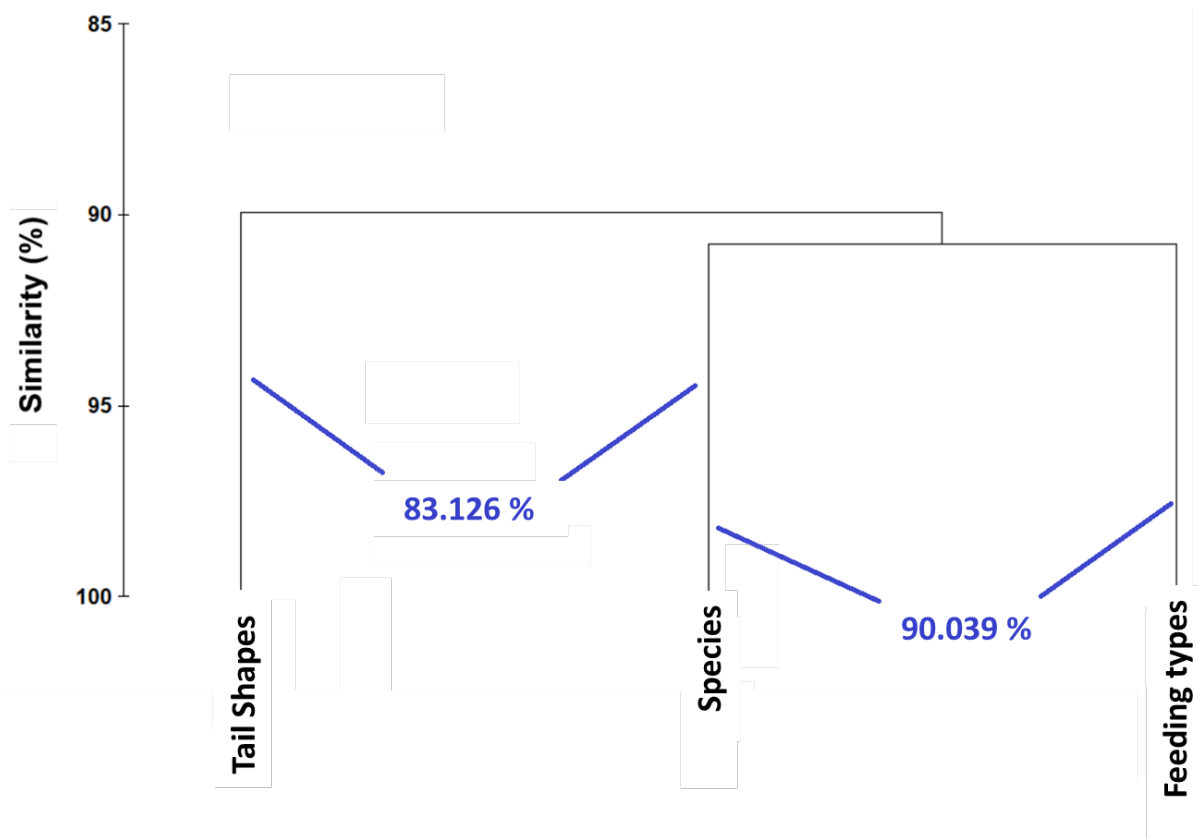
955



957 **Fig. 3.** Changes in the functional traits of nematodes (trophic groups and tail shapes) in the control treatment (UC)
 958 and treatments enriched with amoxicillin [550 ng/L (AMX1) and 1100 ng/L (AMX2)], copper [130 mg/kg Dry
 959 Weight 'dw' (Cu1) and 260 mg/kg dw (Cu2)] and their mixtures (AMX1Cu1, AMX2Cu2, AMX2Cu1, and
 960 AMX1Cu2) over a 30 days period. Visual summary based on relative abundances (A and B), cluster analyses (C
 961 and D), and non-metric multidimensional scaling (nMDS) representations (E and F). Feeding groups: selective
 962 deposit feeders (1A), non-selective deposit feeders (1B), epigrowth feeders (2A), omnivorous-carnivorous (2B).

963 Tail shapes: elongated/filiform (e/f), short/round (s/r), conical (co), clavate/cylindrical (cla). Asterisks above bars
964 indicate significant differences compared to the control groups, according to the Chi-square test results ($\sqrt{-}$
965 transformed data) : $p < 0.05$ (*), $p < 0.01$ (**), $p < 0.001$ (***), $p < 0.0001$ (****).

966



967

968

969 **Fig. 4.** Second-stage clustering based Spearman rank correlations derived from inter-matrix
970 comparisons. Included matrices are those represented in Figures 2 (species composition) and 3
971 (functional traits). Average similarity values are indicated on the dendrogram branches.

972

973

974

975

976

977

978

979

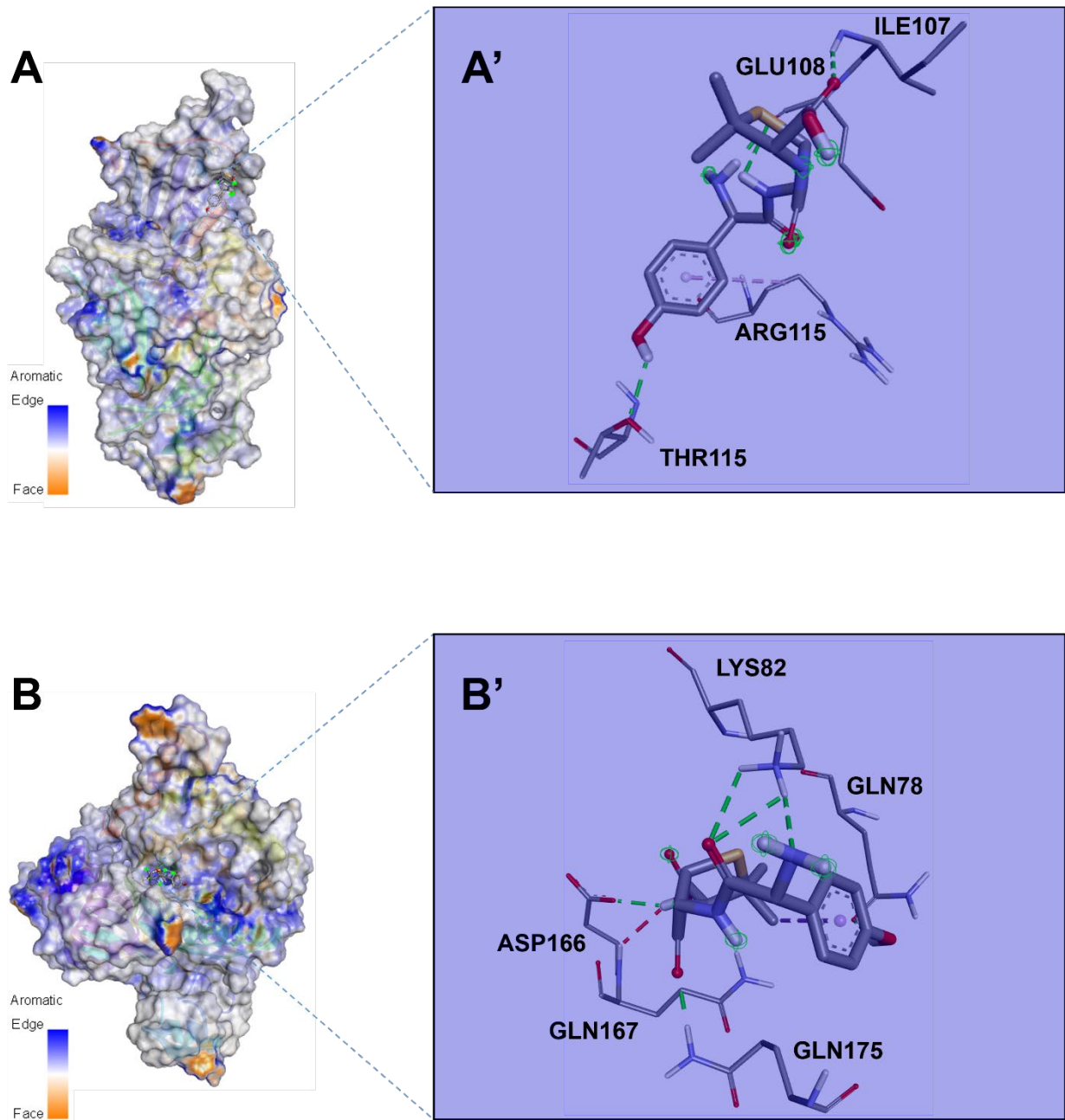
980

981

982

983

984

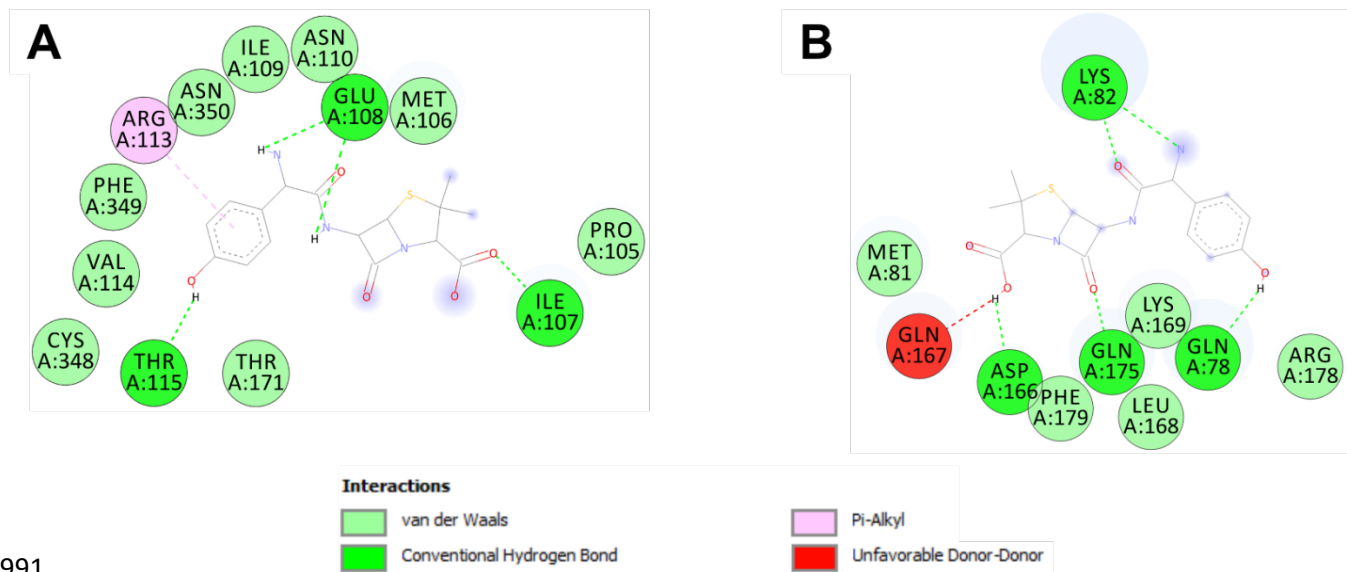


985

986

987 **Fig. 5.** 3D illustrations of amoxicillin complexed with (A) Germline Development Protein 3 (GLD-3) and (B) Sex-
988 Determining Protein (SDP) of *Caenorhabditis elegans*, used as a nematode model. Panels (A') and (B') show the
989 corresponding zoomed-in views of the molecular interactions within each complex.

990



991

992

993 **Fig. 6.** Bidimensional interactions diagrams amoxicillin complexed with **(A)** Germline Development Protein 3

994 **(GLD-3)** and **(B)** Sex-Determining Protein (SDP) of *Caenorhabditis elegans*, used as a nematode model.

995

996

997

998

999

Table 2. List of nematode species and their associated functional traits collected from a pristine site along the coast of Jeddah in Saudi Arabia, on March 17, 2023, across the different microcosms. Tail morphotypes: elongated/filiform (e/f), conical (co), clavate/conical-cylindrical (cla), short/rounded (s/r). Feeding types: selective deposit feeders (1A), non-selective deposit feeders (1B), epigrowth feeders (2A), omnivores-carnivores (2B).

Species	Order	Family	Tail shape	Trophic group
<i>Cinctonema papillata</i>	Desmodorida	Microlaimidae	co	1A
<i>Daptonema conicum</i>	Monhysterida	Xyalidae	cla	1B
<i>Daptonema oxycerca</i>	Monhysterida	Xyalidae	cla	1B
<i>Desmodora pontica</i>	Desmodorida	Desmodoridae	co	2A
<i>Dorylaimopsis timmi</i>	Araeolaimida	Comesomatidae	cla	2A
<i>Eleutherolaimus obtusicaudatus</i>	Monhysterida	Linhomoeidae	co	1B
<i>Halalaimus longicaudatus</i>	Enoplida	Oxystominidae	e/f	1A
<i>Halichoanolaimus balochiensis</i>	Chromadorida	Selachinematidae	cla	2B
<i>Metoncholaimus albidus</i>	Enoplida	Oncholaimidae	cla	2B
<i>Metoncholaimus pristiurus</i>	Enoplida	Oncholaimidae	cla	2B
<i>Oncholaimus campylocercoides</i>	Enoplida	Oncholaimidae	cla	2B
<i>Paracanthonchus sadspitensis</i>	Chromadorida	Cyatholaimidae	co	2A
<i>Paramonhystera pellucida</i>	Monhysterida	Xyalidae	cla	1B
<i>Parodontophora breviseta</i>	Araeolaimida	Axonolaimidae	co	1B
<i>Parodontophora pacifica</i>	Araeolaimida	Axonolaimidae	co	1B
<i>Ptycholaimellus sindhicus</i>	Chromadorida	Chromadoridae	co	2A
<i>Sabatieria falcifera</i>	Araeolaimida	Comesomatidae	cla	1B
<i>Terschellingia communis</i>	Monhysterida	Xyalidae	e/f	1A
<i>Terschellingia longicaudata</i>	Monhysterida	Xyalidae	e/f	1A
<i>Theristus flevensis</i>	Monhysterida	Xyalidae	co	1B
<i>Theristus pertenuis</i>	Monhysterida	Xyalidae	co	1B
<i>Theristus polaris</i>	Monhysterida	Xyalidae	co	1B
<i>Trissonchulus oceanus</i>	Enoplida	Ironidae	s/r	1B
<i>Viscosia macramphida</i>	Enoplida	Oncholaimidae	cla	2B
<i>Viscosia viscosa</i>	Enoplida	Oncholaimidae	cla	2B

Table 3. Relative abundance (\pm SD) of free marine nematodes species from in the control treatment (UC) and in treatments enriched with amoxicillin [550 ng/L (AMX1) and 1100 ng/L (AMX2)] or copper [130 mg/kg Dry Weight 'dw' (Cu1) and 260 mg/kg dw (Cu2)] and their mixtures (AMX1Cu1, AMX2Cu2, AMX2Cu1, and AMX1Cu2) after 30 days of the exposure.

Species	UC	Cu1	Cu2	AMX1	AMX2	AMX1/Cu1	AMX2/Cu2	AMX2/Cu1	AMX1/Cu2
<i>Cinctonema papillata</i>	7.27 \pm 2.98	2.27 \pm 1.05	1.42 \pm 0.43	2.45 \pm 2.19		1.32 \pm 0.50	0.52 \pm 0.91		1.17 \pm 0.60
<i>Daptonema conicum</i>	5.50 \pm 0.11	6.51 \pm 2.36	2.44 \pm 1.34	9.75 \pm 3.34	1.76 \pm 0.99	2.38 \pm 0.58	0.48 \pm 0.83	10.22 \pm 10.32	3.45 \pm 2.74
<i>Daptonema oxycerca</i>	0.88 \pm 0.50	7.30 \pm 2.30	10.27 \pm 1.63	5.20 \pm 2.60	12.42 \pm 0.84	9.48 \pm 1.45			1.62 \pm 1.69
<i>Desmodora pontica</i>	2.14 \pm 0.94	4.59 \pm 2.15	3.55 \pm 2.12	3.87 \pm 0.93	8.99 \pm 2.27	3.73 \pm 0.35	13.60 \pm 2.85	11.91 \pm 4.30	7.39 \pm 2.56
<i>Dorylaimopsis timmi</i>	5.75 \pm 1.88	0.90 \pm 0.83	0.93 \pm 1.62	1.70 \pm 1.35	3.54 \pm 1.53	4.64 \pm 2.10	10.35 \pm 7.33	1.95 \pm 1.88	
<i>Eleutherolaimus obtusicaudatus</i>	8.59 \pm 0.78	5.98 \pm 4.30	9.52 \pm 2.40	8.14 \pm 1.22	7.69 \pm 7.34	8.10 \pm 0.63		5.01 \pm 3.94	8.74 \pm 0.91
<i>Halalaimus longicaudatus</i>	5.33 \pm 2.28	2.96 \pm 0.79	2.17 \pm 0.79	4.26 \pm 3.35	0.55 \pm 0.96				1.50 \pm 1.71
<i>Halichoanolaimus balochiensis</i>	3.79 \pm 0.45	4.67 \pm 1.90	3.11 \pm 1.10	4.47 \pm 1.59	3.91 \pm 3.68	3.25 \pm 0.57	6.87 \pm 7.65	4.20 \pm 3.79	4.22 \pm 4.01
<i>Metoncholaimus albidus</i>	1.70 \pm 0.55	3.65 \pm 2.56	5.07 \pm 1.33	5.30 \pm 0.82	8.00 \pm 2.80	4.77 \pm 0.87	13.65 \pm 3.41		
<i>Metoncholaimus pristiurus</i>	1.48 \pm 0.65	5.90 \pm 1.45	1.44 \pm 0.51	2.56 \pm 0.98	2.98 \pm 1.27	4.57 \pm 1.62	6.62 \pm 5.04	13.95 \pm 2.44	8.10 \pm 2.05
<i>Oncholaimus campylocercoides</i>	2.23 \pm 0.72	1.51 \pm 0.86	4.52 \pm 3.73	2.19 \pm 0.83	3.80 \pm 3.05	2.86 \pm 0.82	14.87 \pm 2.13	8.46 \pm 3.16	0.38 \pm 0.37
<i>Paracanthonus sadspitensis</i>	6.34 \pm 0.65	0.82 \pm 1.43	0.90 \pm 0.88	5.73 \pm 0.78	13.16 \pm 3.33	2.32 \pm 0.48	9.14 \pm 1.69	2.05 \pm 0.43	1.48 \pm 0.73
<i>Paramonhystera pellucida</i>	4.64 \pm 1.11	4.45 \pm 1.14	7.05 \pm 1.50	5.19 \pm 2.68	4.39 \pm 1.58	5.09 \pm 1.09	0.48 \pm 0.83	4.58 \pm 4.12	5.26 \pm 2.23
<i>Parodontophora beviseta</i>	4.46 \pm 1.54	3.22 \pm 0.58	3.55 \pm 0.76	2.77 \pm 0.69	3.37 \pm 0.96	3.61 \pm 0.54	0.24 \pm 0.42	2.73 \pm 0.96	4.65 \pm 1.60
<i>Parodontophora pacifica</i>	4.18 \pm 0.47	3.37 \pm 2.32	4.33 \pm 2.20	4.10 \pm 1.20	1.94 \pm 0.77	5.11 \pm 1.48	1.81 \pm 2.55	2.59 \pm 1.62	5.20 \pm 2.50
<i>Ptycholaimellus sindhicus</i>	0.67 \pm 0.47	4.06 \pm 5.40		3.03 \pm 1.96	3.36 \pm 0.28	5.47 \pm 2.47	6.63 \pm 1.85	1.44 \pm 1.09	2.59 \pm 0.94
<i>Sabatieria falcifera</i>	4.61 \pm 0.49	5.16 \pm 3.22	12.97 \pm 4.45	5.83 \pm 5.80	5.35 \pm 3.44	4.99 \pm 2.24	0.48 \pm 0.83	5.86 \pm 3.27	5.70 \pm 2.47
<i>Terschellingia communis</i>	0.83 \pm 0.31	2.31 \pm 1.31	3.88 \pm 3.12	5.67 \pm 2.83	0.39 \pm 0.64	2.88 \pm 1.20			1.78 \pm 1.94
<i>Terschellingia longicaudata</i>	5.69 \pm 2.74	2.49 \pm 1.08	1.60 \pm 0.73	2.65 \pm 0.62	0.60 \pm 0.62			0.17 \pm 0.30	10.18 \pm 4.76
<i>Theristus flevensis</i>	1.25 \pm 0.09	5.21 \pm 2.41	2.95 \pm 1.36	2.90 \pm 1.07	0.80 \pm 0.38	3.94 \pm 0.86	1.29 \pm 2.24	5.95 \pm 4.35	5.10 \pm 4.66
<i>Theristus pertenuis</i>	6.29 \pm 0.24	5.84 \pm 0.44	4.50 \pm 1.96	1.80 \pm 1.63	1.16 \pm 1.01	4.95 \pm 0.63		2.14 \pm 1.87	5.15 \pm 1.63
<i>Theristus polaris</i>	5.80 \pm 0.72	3.1 \pm 0.56	2.68 \pm 1.56	2.66 \pm 1.36		7.10 \pm 1.70	0.24 \pm 0.42	3.62 \pm 1.75	4.58 \pm 1.90
<i>Trissonchulus oceanus</i>	3.48 \pm 0.39	4.00 \pm 0.66	2.70 \pm 1.61	2.37 \pm 1.50	4.78 \pm 1.25	2.19 \pm 0.66		2.10 \pm 1.89	1.34 \pm 0.85
<i>Viscosia macramphida</i>	2.48 \pm 0.42	5.65 \pm 3.90	3.78 \pm 2.38	3.22 \pm 0.09	6.66 \pm 3.56	3.38 \pm 0.38	4.54 \pm 0.56	4.12 \pm 1.77	3.53 \pm 1.39
<i>Viscosia viscosa</i>	4.58 \pm 0.17	4.08 \pm 2.47	4.68 \pm 3.54	2.20 \pm 0.19	0.41 \pm 0.72	3.88 \pm 0.54	8.18 \pm 2.66	6.94 \pm 2.01	6.90 \pm 2.71

Table 4. Analysis of similarity (ANOSIM) and percent similarity (SIMPER) comparing the control treatment (UC) with treatments enriched with amoxicillin [550 ng/L (AMX1) and 1100 ng/L (AMX2)], copper [130 mg/kg Dry Weight ‘dw’ (Cu1) and 260 mg/kg dw (Cu2)] and their mixtures (AMX1Cu1, AMX2Cu2, AMX2Cu1, and AMX1Cu2). The table provides average dissimilarity (AD) values between treatments based on square root transformed nematode species abundance. Species contributing to approximately 70% of the total dissimilarity are listed in order of their contribution. Symbols: more present (+); less present (-); eliminated (elim).

Comparisons	UC vs. Cu1	UC vs. Cu2	UC vs. AMX1	UC vs. AMX2
ANOSIM	R -statistics = 0.926 p = 0.01	R -statistics = 1 p = 0.01	R -statistics = 0.889 p = 0.01	R -statistics = 1 p = 0.01
SIMPER	AD = 25.92%	AD = 28.70%	AD = 19.37%	AD = 39.33%
	<i>Paracanthochus sadspitensis</i> (10.27%) - <i>Dorylaimopsis timmi</i> (8.76%) - <i>Cincontema papillata</i> (7.75%) - <i>Eleutherolaimus obtusicaudatus</i> (6.28%) - <i>Terschellingia longicaudata</i> (5.73%) - <i>Theristus polioris</i> (5.47%) - <i>Halalaimus longicaudatus</i> (4.91%) - <i>Daptonema oxycerca</i> (4.82%) + <i>Parodontophora breviseta</i> (3.82%) - <i>Theristus pertenuis</i> (3.72%) - <i>Parodontophora pacifica</i> (3.69%) - <i>Viscosia viscosa</i> (3.57%) -	<i>Dorylaimopsis timmi</i> (9.03%) - <i>Paracanthochus sadspitensis</i> (8.97%) - <i>Cincontema papillata</i> (8.35%) - <i>Terschellingia longicaudata</i> (6.58%) - <i>Theristus polioris</i> (5.93%) - <i>Daptonema conicum</i> (5.84%) - <i>Daptonema oxycerca</i> (5.65%) + <i>Halalaimus longicaudatus</i> (5.64%) - <i>Theristus pertenuis</i> (4.88%) - <i>Eleutherolaimus obtusicaudatus</i> (3.77%) - <i>Parodontophora breviseta</i> (3.59%) -	<i>Theristus pertenuis</i> (8.31%) - <i>Cincontema papillata</i> (7.92%) - <i>Dorylaimopsis timmi</i> (7.73%) - <i>Terschellingia communis</i> (6.70%) + <i>Daptonema oxycerca</i> (6.12%) + <i>Theristus polioris</i> (5.77%) - <i>Terschellingia longicaudata</i> (5.09%) - <i>Viscosia viscosa</i> (4.78%) - <i>Halalaimus longicaudatus</i> (4.41%) - <i>Sabatieria falcifera</i> (4.34%) - <i>Metoncholaimus albidus</i> (4.27%) + <i>Ptycholaimellus sindhicus</i> (4.20%) +	<i>Cincontema papillata</i> (9.52%) elim <i>Theristus polioris</i> (8.56%) elim <i>Halalaimus longicaudatus</i> (7.13%) - <i>Theristus pertenuis</i> (7.11%) - <i>Terschellingia longicaudata</i> (6.96%) - <i>Viscosia viscosa</i> (6.85%) - <i>Daptonema conicum</i> (5.70%) - <i>Eleutherolaimus obtusicaudatus</i> (5.12%) - <i>Dorylaimopsis timmi</i> (4.68%) - <i>Parodontophora pacifica</i> (4.44%) -
Comparisons	UC vs. AMX1/Cu1	UC vs. AMX2/Cu2	UC vs. AMX1/Cu2	UC vs. AMX2/Cu1
ANOSIM	R -statistics = 1 p = 0.01	R -statistics = 1 p = 0.01	R -statistics = 1 p = 0.01	R -statistics = 1 p = 0.01
SIMPER	AD = 24.87%	AD = 54.53%	AD = 29.18%	AD = 41.04%
	<i>Terschellingia longicaudata</i> (11.27%) elim <i>Halalaimus longicaudatus</i> (10.98%) elim <i>Cincontema papillata</i> (8.89%) - <i>Daptonema oxycerca</i> (6.84%) + <i>Paracanthochus sadspitensis</i> (6.71%) - <i>Daptonema conicum</i> (5.81%) - <i>Ptycholaimellus sindhicus</i> (4.60%) + <i>Theristus pertenuis</i> (4.08%) - <i>Dorylaimopsis timmi</i> (3.88%) - <i>Eleutherolaimus obtusicaudatus</i> (3.86%) - <i>Metoncholaimus pristiurus</i> (1.91%) +	<i>Eleutherolaimus obtusicaudatus</i> (8.35%) elim <i>Theristus pertenuis</i> (7.14%) elim <i>Cincontema papillata</i> (7.00%) - <i>Terschellingia longicaudata</i> (6.60%) elim <i>Theristus polioris</i> (6.43%) - <i>Halalaimus longicaudatus</i> (6.43%) elim <i>Daptonema conicum</i> (6.09%) - <i>Paramonhystera pellucida</i> (5.53%) - <i>Parodontophora breviseta</i> (5.52%) - <i>Sabatieria falcifera</i> (5.52%) - <i>Trissonchulus oceanus</i> (5.30%) elim	<i>Dorylaimopsis timmi</i> (10.54%) elim <i>Cincontema papillata</i> (8.52%) - <i>Paracanthochus sadspitensis</i> (7.44%) - <i>Halalaimus longicaudatus</i> (7.03%) - <i>Metoncholaimus albidus</i> (5.69%) elim <i>Daptonema conicum</i> (5.05%) - <i>Oncholaimus campylocercoides</i> (4.99%) - <i>Trissonchulus oceanus</i> (4.74%) - <i>Theristus pertenuis</i> (4.12%) - <i>Theristus polioris</i> (4.06%) - <i>Theristus flevensis</i> (3.85%) + <i>Eleutherolaimus obtusicaudatus</i> (3.80%) -	<i>Cincontema papillata</i> (9.18%) elim <i>Halalaimus longicaudatus</i> (7.75%) elim <i>Terschellingia longicaudata</i> (7.45%) - <i>Dorylaimopsis timmi</i> (5.83%) - <i>Theristus pertenuis</i> (5.80%) - <i>Paracanthochus sadspitensis</i> (5.71%) - <i>Eleutherolaimus obtusicaudatus</i> (5.70%) - <i>Metoncholaimus albidus</i> (4.43%) elim <i>Theristus polioris</i> (4.39%) - <i>Trissonchulus oceanus</i> (4.00%) - <i>Paramonhystera pellucida</i> (3.85%) - <i>Parodontophora pacifica</i> (3.82%) -

Table 5. Analysis of similarity (ANOSIM) and percent similarity (SIMPER) comparing the control treatment (UC) with treatments enriched with amoxicillin [550 ng/L (AMX1) and 1100 ng/L (AMX2)], copper [130 mg/kg Dry Weight ‘dw’ (Cu1) and 260 mg/kg dw (Cu2)] and their mixtures (AMX1Cu1, AMX2Cu2, AMX2Cu1, and AMX1Cu2). The table reports average dissimilarity (AD) values between treatments based on square-root transformed abundances of trophic and tail shape groups. Functional groups contributing to approximately 70% of the total dissimilarity are listed in order of their contribution. Tail shapes: elongated/filiform (e/f), conical (co), clavate/conical-cylindrical (cla), short/rounded (s/r). Feeding types: selective deposit feeders (1A), non-selective deposit feeders (1B), omnivores–carnivores (2B). Symbols: more present (+); less present (-); eliminated (elim).

Comparisons		UC vs. Cu1	UC vs. Cu2	UC vs. AMX1	UC vs. AMX2
Trophic groups	ANOSIM	AD = 15.91% <i>R</i> -statistics = 0.667 <i>p</i> = 0.01	AD = 19.90% <i>R</i> -statistics = 0.63 <i>p</i> = 0.01	AD = 8.79% <i>R</i> -statistics = 0.185 <i>p</i> = 0.01	AD = 26.11% <i>R</i> -statistics = 0.852 <i>p</i> = 0.01
	SIMPER	2B (28.86) + 1A (28.54) -	1B (33.32) + 1A (25.26) -	1B (34.65%) + 1A (31.84%) -	1A (33.71%) - 2B (27.06%) +
Tail shapes	ANOSIM	AD = 15.32% <i>R</i> -statistics = 0.667 <i>p</i> = 0.01	AD = 19.39% <i>R</i> -statistics = 0.63 <i>p</i> = 0.01	AD = 12.71% <i>R</i> -statistics = 0.185 <i>p</i> = 0.01	AD = 16.87% <i>R</i> -statistics = 0.852 <i>p</i> = 0.01
	SIMPER	cla (40.51%) + co (40.22%) - e/f (16.98%) -	cla (47.98%) + co (35.14%) - e/f (13.94%) -	cla (39.11%) + co (37.63%) - e/f (17.89%) -	cla (46.13%) + e/f (30.61%) - co (19.39%) -
Comparisons		UC vs. AMX1/ Cu1	UC vs. AMX2/Cu2	UC vs. AMX1/Cu2	UC vs. AMX2/Cu1
Trophic groups	ANOSIM	AD = 8.79% <i>R</i> -statistics = 1 <i>p</i> = 0.04	AD = 63.26% <i>R</i> -statistics = 1 <i>p</i> = 0.01	AD = 9.23% <i>R</i> -statistics = 0.1 <i>p</i> = 0.01	AD = 26.54% <i>R</i> -statistics = 0.667 <i>p</i> = 0.01
	SIMPER	1A (47.47%) -	1B (35.30%) - 2B (30.41%) +	2B (37.19%) + 1A (24.30%) -	2B (40.33%) +
Tail shapes	ANOSIM	AD = 12.66% <i>R</i> -statistics = 1 <i>p</i> = 0.01	AD = 26.37% <i>R</i> -statistics = 1 <i>p</i> = 0.03	AD = 6.51% <i>R</i> -statistics = 1 <i>p</i> = 0.01	AD = 24.60% <i>R</i> -statistics = 0.667 <i>p</i> = 0.01
	SIMPER	cla (45.99%) + e/f (35.44%) - co (13.48%) -	cla (50.00%) + co (22.44%) - e/f (22.21%) -	co (31.61%) - cla (26.19%) + e/f (25.76%) - s/r (16.44%) -	cla (49.77%) + e/f (24.07%) elim co (22.37%) -

Table 6. Binding affinities and closest interacting residues of amoxicillin with Germline Development Protein 3 (GLD-3) and Sex-Determining Protein (SDP) of *Caenorhabditis elegans*.

Entry	Affinity (kcal/mol)	RMSD (lower-upper)	Interacting Residues (distance, Å)	Closest Interacting Residue
GLD-3	-6.4	0.0-36.10	Conventional H-Bond: ILE107 (2.682), GLU108 (2.962), GLU108 (1.994), THR115 (2.189)	GLU108:O
			π-Alkyl: ARG113	
SDP	-7.7	0.0-32.39	Conventional H-Bond: LYS82 (2.711), LYS82 (2.711), LYS82 (2.935), GLN175 (1.875), ASP166 (2.118), GLN78 (2.263)	GLN175:HE21